

Holocene tufa in the Slovak Karst: facies, sedimentary environments and depositional history

Michał GRADZIŃSKI¹*, Helena HERCMAN², Martyna JAŚKIEWICZ¹ and Stanisław SZCZUREK¹

¹ Institute of Geological Sciences, Jagiellonian University, Oleandry 2a, 30-063 Kraków, Poland

² Institute of Geological Sciences, Polish Academy of Sciences, Twarda 51/55, 00-818 Warszawa, Poland



Gradziński M., Hercman H., Jaśkiewicz M. and Szczurek S. (2013) Holocene tufa in the Slovak Karst: facies, sedimentary environments and depositional history. *Geological Quarterly*, 57 (4): 769–788, doi: 10.7306/gq.1131

Several tufa complexes are known in the Slovak Karst which is a typical karst area of a temperate climate. This area is built of Mesozoic carbonates, mainly Triassic in age. The karst systems drain carbonate plateaux and lead water to resurgences located in valleys which are up to 300 m deep. Below the resurgences there are Holocene fossil tufa deposits that exceed 12 m in thickness. The tufas include stromatolite, moss, phytoclastic, oncoidal, and intraclastic facies. Extensive barrages which once dammed the upper reaches of the streams were formed in narrow valleys. They are composed predominantly of moss facies and stromatolites, with subordinate oncoidal and phytoclastic facies. Phytoclastic, oncoidal and intraclastic facies are dominant in dammed segments of streams, and include gastropod shells and charcoal fragments. Some small moss cushions are also developed. Barrages and dammed areas formed in a longitudinal fluvial depositional system. Conversely, below resurgences located on plateau slopes tufas of a perched springline depositional system were formed. These comprise deposits of prograding cascades constructed by moss, phytoclastic and stromatolitic facies. Presently, the tufas analysed are inactive. They stopped growing in the Late Holocene time, after which there was abrupt incision of the streams. This caused downcutting into Holocene tufas, in some places reaching Mesozoic bedrock. At present tufa is being precipitated from streams in all the sites studied.

Key words: fluvial tufa, perched springline tufa, radiocarbon dating, Quaternary, Late Holocene tufa decline, Central Carpathians.

INTRODUCTION

Freshwater carbonates are deposited near springs worldwide (Ford and Pedley, 1996; Pentecost, 2005). The term tufa is used to denote such deposits if they comprise macro- or microphyte moulds or imprints (Pedley, 2009). However, some authors extend the meaning of the term “travertine” to such deposits (see Gandin and Capezuoli, 2008 as well as Jones and Renaut, 2010, for terminological discussion). Tufas are predominantly fed by shallowly circulating meteoric water charged with biogenic CO₂ of soil origin.

Tufas form an important palaeoenvironmental archive, and lately there has been a rapid increase in the number of publications dealing with this deposit type. Tufas are used in reconstructing palaeoclimate – chiefly temperature and humidity which influence vegetation type, as well as geomorphic evolution, palaeohydrology, tectonics and even the activity of the prehistoric humans (e.g., Pazdur et al., 1988a; Peña et al., 2000; Soligo et al., 2002; Martín-Algarra et al., 2003; Andrews and Brasier, 2005;

Andrews, 2006; Anzalone et al., 2007; Capezuoli et al., 2010; Mastella and Rybak-Ostrowska, 2012; Arenas et al., 2013). Sections of fossil tufa have been studied in detail by means of stable isotopes (mainly carbon and oxygen), geochemistry, molluscs and plant remains, including pollen (e.g., Taylor et al., 1998; Vermoere et al., 1999; Meyrick and Preece, 2001; Ihlenfeld et al., 2003; Garnett et al., 2004), to reconstruct several characteristic parameters of the palaeoenvironment.

Conversely, factors controlling the variation and distribution of tufa facies in space and time have been studied less extensively. Pentecost and Viles (1994) and Pentecost (2005: p. 49–76) described and classified the geometry of growing tufa structures. Pedley (1990), Ford and Pedley (1996) and Pedley et al. (1996, 2003) studied facies systems (models) and interpreted their sedimentary environment. Pedley et al. (1996) proposed two different facies models for cool temperate and warm semi-arid fluvial tufas. Carthew et al. (2003) analysed deposits from northwestern Australia and noted several differences between temperature and tropical climate tufas, such as a lack of oncoids, occurrence of abundant larval housings and sunken rafts in the latter ones. Viles et al. (2007) studied tufa from an arid region of Africa and recorded differences between the development of fluvial tufa in different climatic zones. Arenas-Abad et al. (2010), Vázquez-Urbez et al. (2012) and Arenas et al. (2013) described facies sequences and sedimentary models of Holocene and Pleistocene tufa systems in Spain and discussed

* Corresponding author, e-mail: michal.gradzinski@uj.edu.pl

their depositional environment in detail. Several facies types of spring-associated tufas and their depositional settings have been recognized in the Eastern Alps (Sanders and Werl, 2011). Keppel et al. (2011) interpreted the facies development of a tufa mound spring fed by artesian water in South Australia. One can expect that such aspects will be of concern to the geological community in the future as will be the implications of the discovery of oil and gas in the South Atlantic region within freshwater limestone probably, at least partly, of spring-fed type (Harris et al., 2013).

Fossil tufa outcrops and sites of modern tufa deposition widely occur across the Slovak Karst area. Kovanda (1971) listed 23 localities with fossil or modern tufa and, more recently, Kilík (2008) described and illustrated 20 tufa localities. Tufa has long been utilized in this area e.g., as building stone for the local medieval castle (Fig. 1).

Some tufa deposits in this region were recognized in the 19th and the beginning of the 20th century (Hochstetter, 1856; Vitális, 1909). Subsequently, Kormos (1912) described in more detail tufa from the Háj, Hrhov and Hrušov localities and focused especially on their preserved molluscs. He regarded these deposits as Pleistocene in age and stressed also that their growth had ceased while, later on, those tufas were subjected to erosion. The mollusc content of seven localities, including Háj, Hrhov and Gombasek were studied by Petrboš (1937), who indicated a Holocene age for the tufas studied, as confirmed by finding Neolithic pottery at Háj and Hrhov and in line with palaeobotanical studies by Němejc (1936, 1944). The Háj and Hrhov localities were most closely studied by Ložek (1955, 1958) who described several taxa of snails and, subordinately, bivalves. The tufa studied contained also pottery of Hallstatt culture affinity. The Holocene age of the tufa at Háj was further supported by an exploratory ^{14}C date (Gradziński, 2010). Although tufa in the Slovak Karst has been studied in terms of molluscs and palaeobotany, neither its facies nor sedimentary environment, nor its age were precisely determined.

The present study deals with selected Holocene tufa deposits from the Slovak Karst area. The aim is to recognize tufa facies architecture and decipher factors controlling facies variation. Another goal is to establish the chronology of tufa growth based on the reconstruction of the spatial arrangement of facies, integrated with ^{14}C dating results and to investigate the cessation of tufa growth in the late Holocene in the Slovak Karst.



Fig. 1. Lintel constructed of resistant tufa facies in the medieval castle at Turňa nad Bodvou

GEOLOGICAL SETTING

The Slovak Karst area located in eastern Slovakia is a typical upland karst, comprising several karst plateaux. Their altitude ranges from about 400 to 800 m whereas intervening valleys are located at about 200–300 m. The plateaux are formed of various Triassic carbonates, namely of Wetterstain, Steinalm, Gutenstein and Hallstatt types, belonging to the Silica Nappe (Fig. 2; Mello, 1996). Lower Triassic clastic deposits occur subordinately. Craggs and ridges of Triassic carbonates occur on steep slopes of the plateaux whereas dolinas with sinkholes and blind valleys are developed on the plateau surfaces. Plateau tops and some slopes are partly covered by deciduous forests. South-facing, steep, partly rocky slopes of plateaux are covered by xerothermic grasslands and bushes.

At the foot of the plateaux several karst springs are situated. These drain the plateaux through extensive cave systems. The present average discharge of the springs reaches 120 l/s (Jakál and Bella, 2008). Presently, tufas are being formed in headwater streams (Kovanda, 1971; Kilík, 2008; Gradziński, 2010), adjacent to inactive tufa deposits. Most are exposed by erosional cuts several metres deep.

Three different inactive tufa successions, namely those of Háj, Hrhov and Gombasek, have been selected for this study. They differ in location, thickness and facies types.

Tufa of the Háj Valley (in Slovak – the Hájska dolina) stretches for 900 m northwards of the village of Háj. The valley is narrow and it is incised to a depth ca. 150–200 m into the surrounding carbonate plateaux (Figs. 3A and 4A). The head segment of the valley is carved into the Bôrka Nappe which comprises metabasites, phyllites and shales as well as limestones. The bottom part of the valley is partly filled with tufa, which in turn is downcut to the Mesozoic bedrock. Tufa terraces are preserved on both sides of the valley, tufa sections cropping out on terrace slopes. The present stream is fed by a series of karst springs located at the valley bottom. It forms four waterfalls, each a few metres high, developed in places where relatively resistant tufa types build a basement. Modern tufa is being formed in the stream (Gradziński, 2010). It forms picturesque curtains on the waterfall faces and builds some small barrages in the stream (Fig. 4B).

Tufa at Hrhov is located on the bottom of plateau slopes, at altitudes of around 220–230 m (Figs. 3B and 4C). The highest points on the plateau exceed 800 m in height whereas the wide, flat bottom of the Turňa Basin is located roughly at 190–200 m. The tufa was fed by the Veľká hlava (in Hungarian – the Félj) spring, which is situated on the plateau slope at an altitude of around 240 m, around 40 m above the valley bottom. Such a location is caused by the occurrence of relatively impermeable layers of Lower Triassic clastic rocks below Middle Triassic carbonates, which effectively pond groundwater. The slopes above the spring are composed exclusively of Triassic carbonates. The spring is fed by autogenic water derived from the top of the neighbouring karst plateau. Hydrological connection with a vertical cave situated on the plateau has been demonstrated (Jakál and Bella, 2008).

Tufa outcrops at Hrhov were extensively exploited as early as in the beginning of the last century (Němejc, 1936; Ložek, 1958). Several old buildings in the village, local churches included, are built of tufa. Presently, the former exploitation area has been built on, houses occupying the old, abandoned quarries. On the wall of the largest quarry there is a waterfall showing extensive growth of tufa curtains (Kilík, 2008).

Tufa at Gombasek has been studied near the Black Resurgence (in Slovak – the Čierna vyvieracka), which drains a resur-

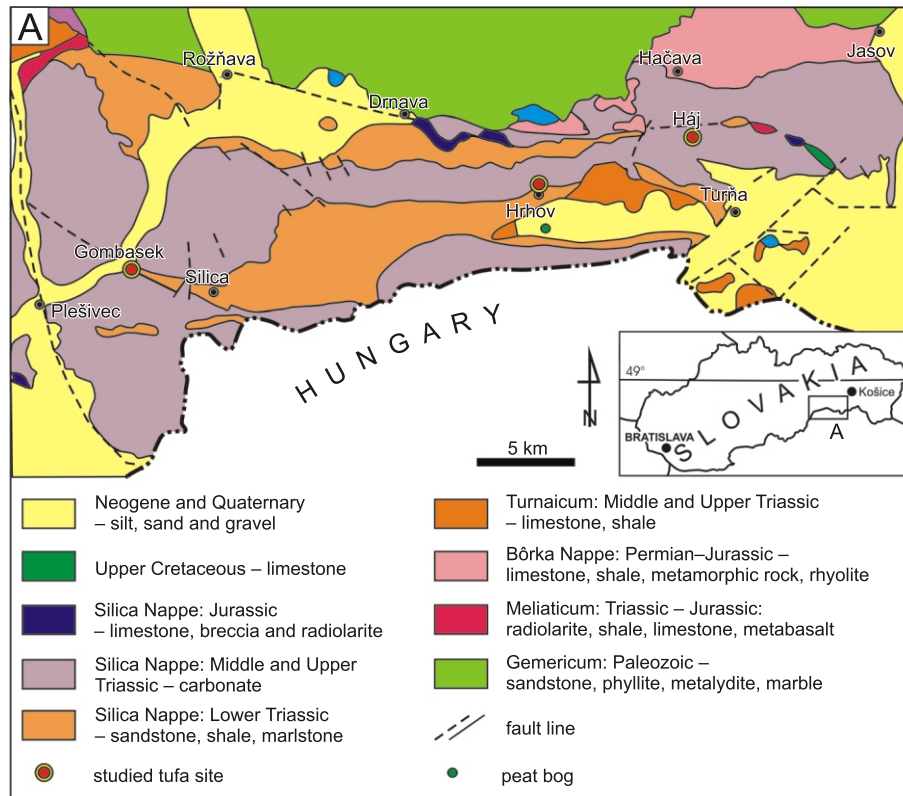


Fig. 2. Geological map of the Slovak Karst area with location of the tufa sites studied (after Mello et al., 1996, simplified)

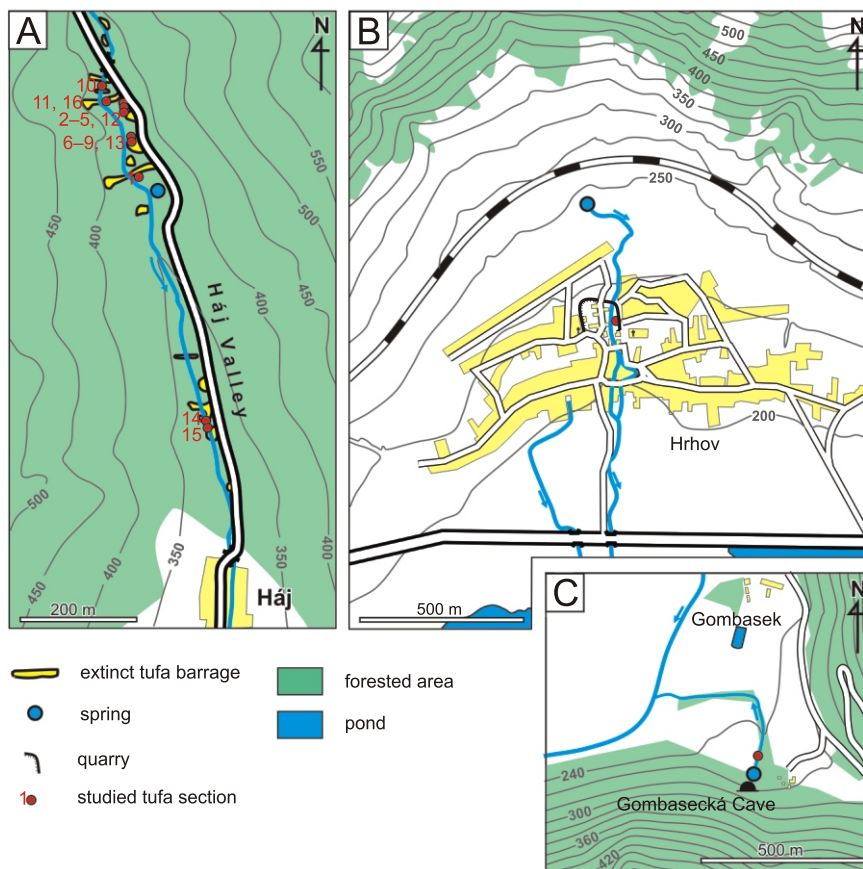


Fig. 3. Location of the tufa sites studied

A – Háj, B – Hrhov, C – Gombasek

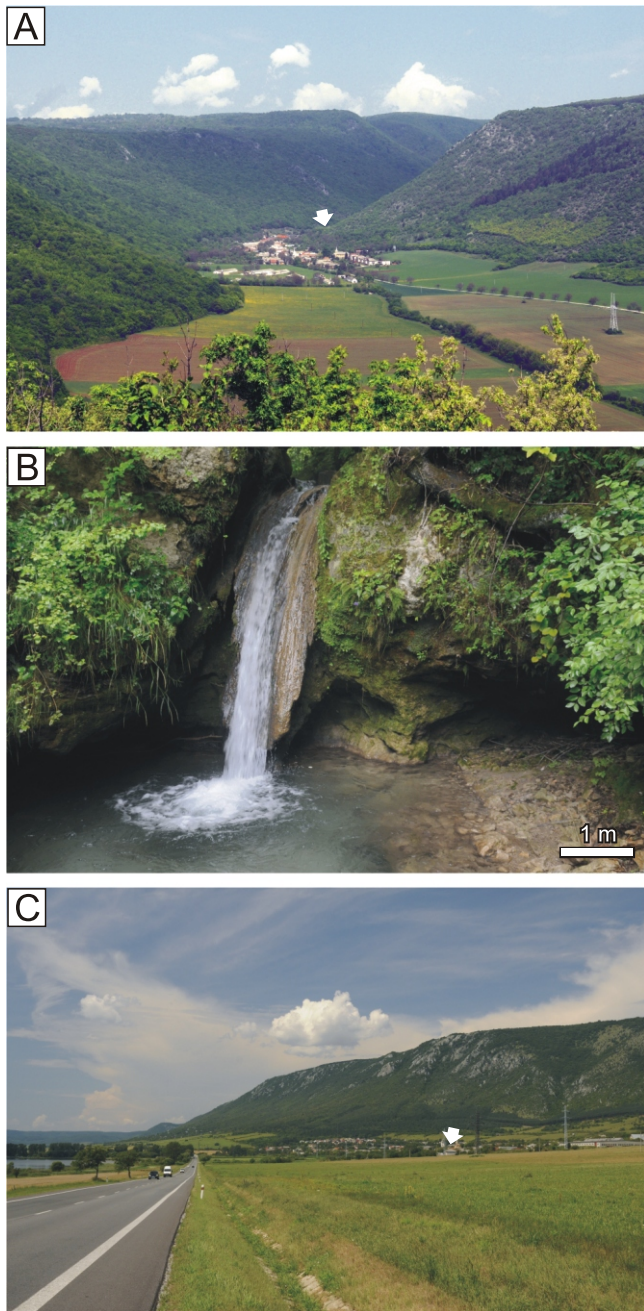


Fig. 4. Sites studied

A – Háj Valley seen from the south, arrow indicates location of tufa upstream of the village of Háj which is situated in the mouth of the valley; **B** – waterfall with active tufa deposition, tufa curtain hangs down from the waterfall head, 5 m high waterfall is developed in the partly eroded old tufa barrage, **C** – village of Hrhov seen from the Turňa Basin, position of tufa is arrowed

gence cave called Gombasecká jaskyňa. The spring is located at an altitude of 238 m about 11 m over the level of the neighbouring Slana River (Fig. 3C). It is situated at the mouth of a wide, dry valley cut into plateau slopes composed of Triassic carbonates, and subordinate Lower Triassic siliciclastic rocks. Several dye-tracer tests have demonstrated connection of the spring with sinkholes and caves on the plateau top (Bella, 2003; Haviarová et al., 2012 and literature quoted therein). Some of the sinkholes are located at the boundary between Lower Triassic siliciclastic rocks and Middle Triassic carbonates. Thus, the spring yields mixed autogenic-allogenic waters.

The stream flowing out from the spring occupies a small canyon-like ditch eroded into older tufas. They are exposed on terrace risers, especially in the walls of a small, presently inactive quarry. The stream has been presently depositing some tufa in the form of small stromatolitic barrages and numerous oncoids.

METHODS

The tufa successions selected for this study were investigated for representative sections which, in turn, were analysed bed-by-bed. Sixteen sections were studied in the Háj Valley and two others at Hrhov and Gombasek (Fig. 3; Appendix 1). The orientation of trunk and branch moulds was measured. The facies were distinguished on their macroscopic characteristics extended by microscopic observations using a standard petrographic microscope and a scanning electron microscope (SEM) Hitachi S-4700 coupled with a Vantage microprobe (Noran product) at the Institute of Geological Sciences, Jagiellonian University. Some samples were etched in 2% HCl before SEM examination.

Geochemical analyses were carried out at ACME Labs (Vancouver, Canada). ICP-emission spectrometry was used to detect the content of Si, Al, Fe, Na, K and Ti. Calcium carbonate contents were measured with calcimeter (Eijkelkamp product), which is based on Scheibler's method. The measurements were conducted at the Institute of Geological Sciences, Jagiellonian University, Kraków. The mineral composition of the tufa was analysed by powder X-ray diffractometry (XRD) using a vertical XPert APD Philips goniometer (PW 1830) at the Institute of Geological Sciences, Jagiellonian University.

Radiocarbon dating of six charcoal samples and eight terrestrial snail shell samples was carried out at the Poznań Radiocarbon Laboratory (Poland) using the AMS method. Pretreatment procedures of organic samples followed those used in the Oxford Radiocarbon Accelerator Unit, as described by Brock et al. (2010). Shell samples, after removal of the outer carbonate layer (ca. 30%) by 0.5M HCl were treated in 15% H₂O₂ (for 10 min in an ultrasonic bath), the remaining carbonate being leached with concentrated H₃PO₄ in a vacuum line. Carbon dioxide produced by combusting organic samples or dissolving carbonate shells was reduced to carbon (Czemik and Goslar, 2001). The content of ¹⁴C in a sample of carbon was measured using the "Compact Carbon AMS" spectrometer produced by the National Electrostatics Corporation, USA (Goslar et al., 2004). Conventional ¹⁴C age was calculated using correction for isotopic fractionation (according to Stuiver and Polach, 1977).

Radiocarbon dating of three carbonate samples was carried out at the Laboratory of Absolute Dating in Skala, Poland. Carbon dioxide, obtained by acid treatment, was converted to benzene. Radiocarbon concentration measurements were conducted using the scintillation technique by a low-background liquid scintillation counter of a new generation, HIDEX 300 SL (Krapiec and Walanus, 2011). The radiocarbon dates obtained were calibrated using the OxCal program (Bronk Ramsey, 2009) and IntCal09 calibration data (Reimer et al., 2009).

Age-depth models were constructed using MOD-AGE software (Hercman and Pawlak, 2012). MOD-AGE uses the randomisation method (a type of Monte Carlo simulation) for age-depth model construction and its confidence band estimation, and the LOESS method for fitting of an age-depth function. The model obtained takes into consideration not only uncertainty of age, but also uncertainty of depth determinations and utilizes all the information from age and depth distributions. Depth uncertainties for model construction were assumed at the ±10 cm level (assuming a normal distribution).

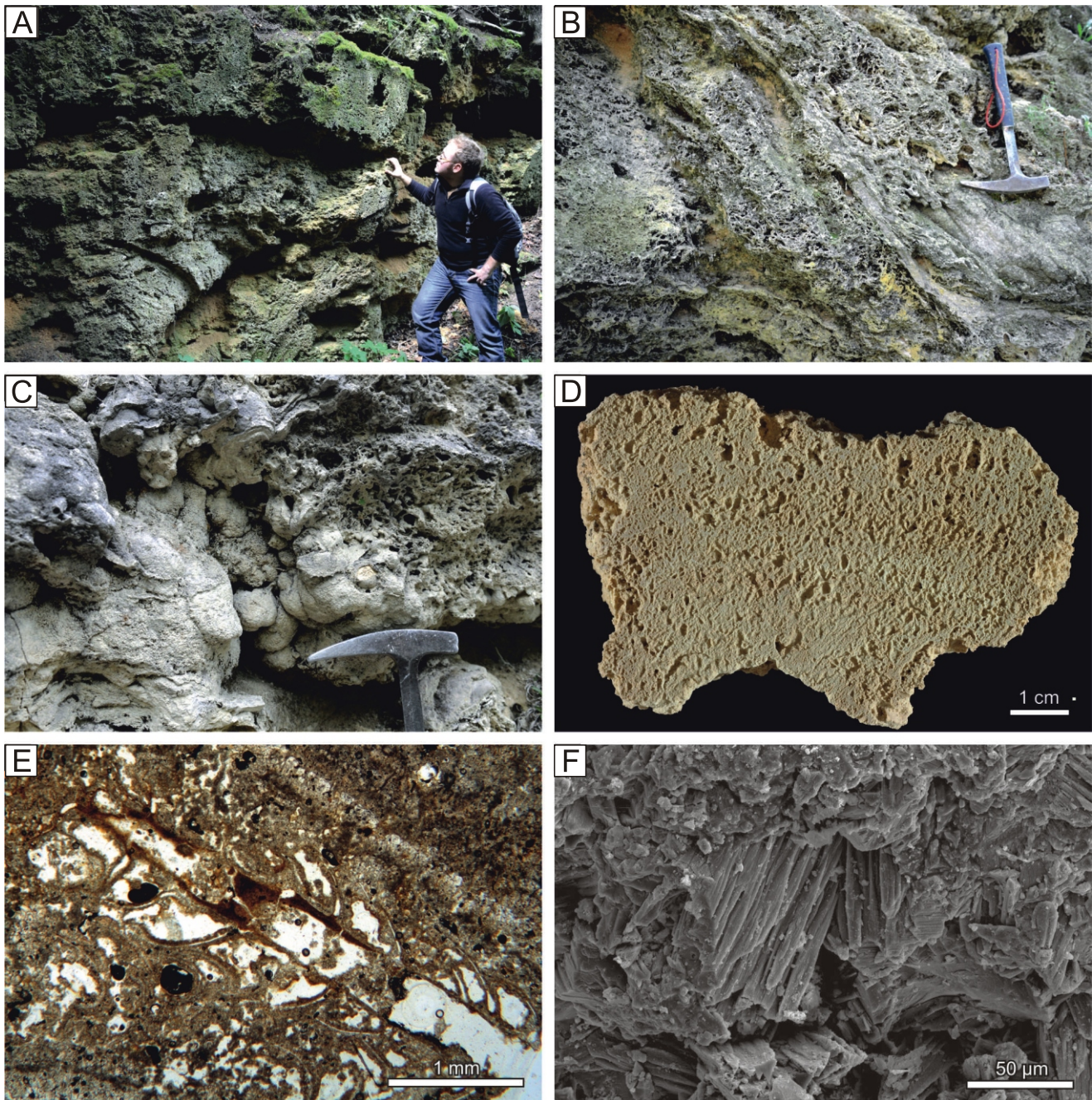


Fig. 5. Moss tufa

A – layered moss tufa, Gombasek; **B** – highly porous moss tufa interlayered with stromatolitic tufa, tufa barrage, Háj, hammer handle is 33 cm long; **C** – cauliflower-shaped knobs encrusting moss tufa; knobs were developed within a cavity below a barrage rim, stromatolite is visible in the upper part of the photograph, Háj, hammer head is 17 cm long; **D** – moss tufa, cross-section, primary porosity is partly reduced by sparry cement, Hrhov; **E** – moss stem entombed with calcite, thin section, Gombasek; **F** – calcite spar-filled porosity in moss tufa, SEM image, Hrhov

RESULTS AND INTERPRETATION

TUFA FACIES

Five tufa facies and one additional facies have been recognized within the tufas studied.

MOSS TUFA

Moss tufa is one of the most common facies in the sections studied (Fig. 5). It represents boundstones composed of calcite-encrusted moss stems and leaves which build three-dimen-

sional, reticulate fabrics (Fig. 5B, D). Moss tufa forms distinct beds, the thickness of which varies from a few centimetres up to 1 m (Fig. 5A, B). Some layers display convex-up upper surfaces. This facies also builds irregular lenses up to 1 m thick and exceeding 3 m in lateral extent.

Moss tufa is hard but friable. Moss stems are mostly oriented parallel to each other but in some cases they are randomly distributed. Parallel-oriented stems are aligned horizontally or subhorizontally (Fig. 5B). Leaf moulds, and snail shells occur subordinately within this facies.

Moss tufa facies is characterized by high primary porosity. The pores exist between neighbouring moss stems which are

encrusted with calcite (Fig. 5E). Some are partly filled with sparry calcite crystals or internal fine-grained calcite sediment (Fig. 5D, F). In larger growth cavities occurring within this facies, cauliflower-shaped knobs coat and link individual moss stems (Fig. 5C). They are composed of sparry crystals and can be classified as speleothems.

Interpretation. Calcite-encrusted mosses are noted from many modern and ancient tufa deposits (e.g., Weijermars et al., 1986; Gradziński et al., 2001; Turner and Jones, 2005). They are an important component of a wide range of tufa-depositing environments, from stagnant palustrine zones to fast-flowing segments of streams (Pedley, 1990). The parallel arrangement of moss stems in the tufas discussed indicated flowing water during deposition. The mosses were encrusted either submerged or via water droplets in a splash zone near cascades or rapids (Pentecost, 2005: p. 237). Being subject to encrustation, moss grows particularly efficiently (Pentecost, 1998). Mosses construct phytoherms of various size, from small moss cushions to large barrages (Pedley, 1990; Pedley et al., 2003; Vázquez-Urbez et al., 2012).

Cauliflower-shaped knobs grew on the outer faces of barrages, commonly below overhangs (see Irion and Müller, 1968; Szulc, 1983; Pentecost, 1999: fig. 4a). They were probably not flushed with water but were located in splash zones being fed by water droplets. Thus, they are morphologically and genetically akin to cave coralloids (see Hill and Forti, 1997: p. 59–62, and literature quoted therein).

STROMATOLITIC TUFA

Tufa stromatolites form beds and lenses ranging from 1 cm to more than 15 cm in thickness (Figs. 5B and 6A). Stromatolites display various orientations, from sub-horizontal, slightly undulated to deeply inclined. They mirror the basement geometry (Figs. 5B and 6A, see Fig. 11). They comprise lighter and darker laminae which alternate with each other (Fig. 6B, C). The laminae differ in porosity, and are up to 0.9 mm in thickness. Microscopic (petrographic and SEM) observations show various moulds of cyanobacterial and algal filaments within the stromatolites (Fig. 6F–H).

Larval housings are very common within the stromatolitic tufa studied (Fig. 6D, E). They dominate in some laminae, and build meandering networks. As a rule, their ceilings are composed of thin, convex-up micritic laminae, which are overlain by sparry cements.

Interpretation. Stromatolites occur in tufas all over the world. The range of microbial involvement in their growth in a tufa depositional milieu is a matter of debate. Some authors suggest that cyanobacteria and algae actively contribute to the precipitation of the carbonates forming tufa stromatolites (e.g., Shiraishi et al., 2008; Pedley et al., 2009; Gradziński, 2010) while others imply that they only provide a suitable substrate for carbonate mineral nucleation (e.g., Merz-Preiß and Riding, 1999; Pentecost and Whitton, 2000). Stromatolites may be formed either in almost stagnant water or in fast-flowing streams. The inclination of some of the stromatolitic beds studied suggests they littered steep stream-beds, indicating the lat-

ter. This is supported by the common occurrence of larval housings within stromatolites since analogous larval housings have been: (1) found in many recent tufas which originate in fast-flowing water settings (Drysdale, 1999; Janssen et al., 1999; Šemnički et al., 2012), including the Háj Valley (Gradziński, 2010), and (2) are recognized in high-energy fossil tufas, especially in warm climate zones (Carthew et al., 2003).

PHYTOCLASTIC TUFA FACIES

This facies comprises phytoclasts encrusted with calcium carbonate (Figs. 6A and 7). At present, phytoclasts are decomposed and empty moulds of plants are surrounded by carbonate coatings. The phytoclasts range from trunks up to 0.5 m in diameter through branches to small twigs and leaves. The encrustations around phytoclasts are up to a few millimetres in thickness. They are of stromatolitic type since they are laminated and comprise cyanobacterial and algal moulds, as well as a few larval housings (Fig. 7F). The spatial organization of encrustations around phytoclasts differs from the stromatolitic tufa described above, as the latter builds individual layers. However, encrustations in some cases grade upwards into a massive stromatolitic cover (Fig. 6A). In situ encrusted plants in life positions occur subordinately within the phytoclastic tufa (Fig. 7B). Phytoclastic tufa facies includes some snail shells as a minor component. This facies forms layers and lenses up to 0.5 m thick.

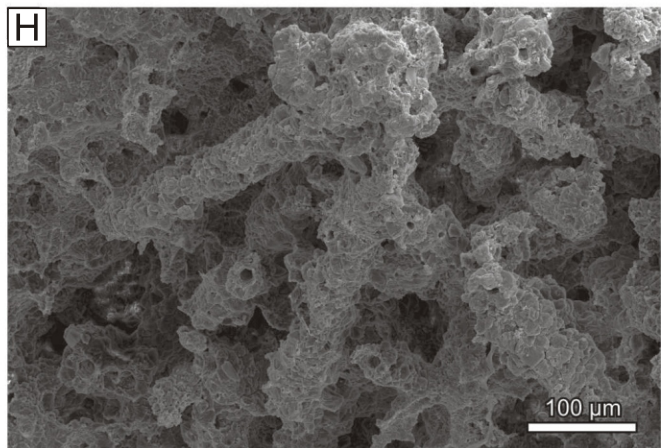
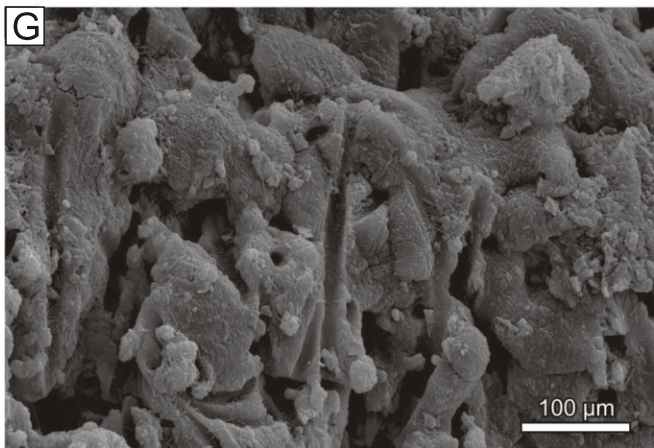
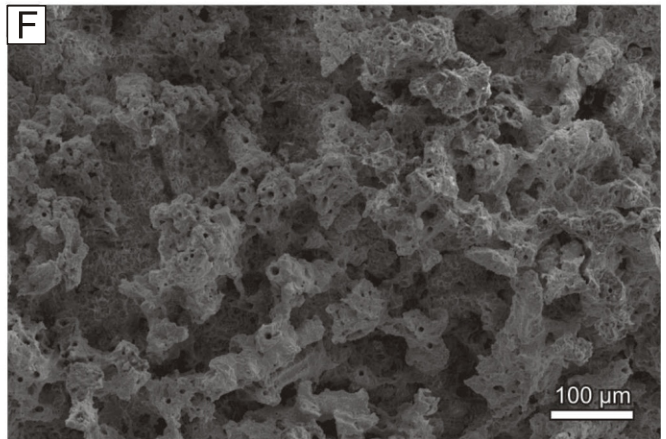
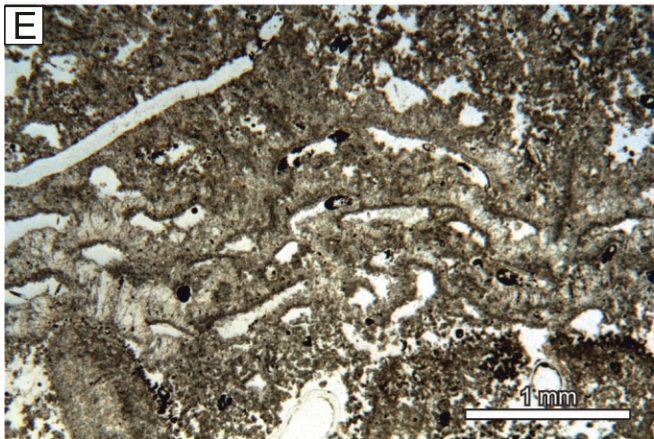
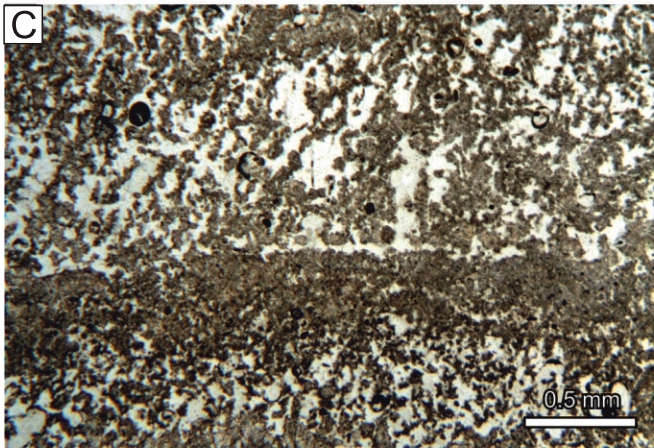
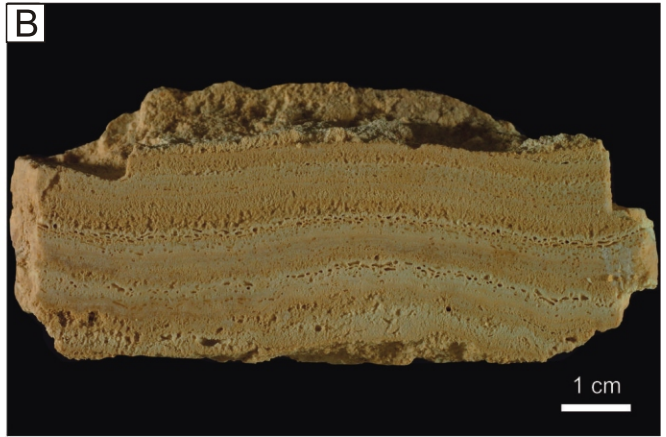
Interpretation. The phytoclasts owe their origin to erosion of plants upstream of the deposition loci. They may be derived from shallow zones of a stream or from a palustrine zone or even an adjoining land area. The last of these is confirmed by the presence of land plant detritus, such as tree trunks, stems and leaves as well as land snail shells within the facies discussed in all the sites studied (Fig. 7A–E; see also Nêmejc, 1936; Petrbok, 1937; Ložek, 1955, 1958). Phytoclasts were transported as pure plant debris or were at least partly incrustated before their deposition (Vázquez-Urbez et al., 2012; García-García et al., 2013). Although the empty plant moulds are the most visible elements of phytoclastic tufa, this facies originated in situ. It is not an accumulation of formerly encrusted plant detritus (see Pedley, 1990; Glover and Robertson, 2003). Hence, it represents a specific type of boundstone. The deposition of this facies resulted from high-energy episodes, probably of flash-flood type and subsequent encrustation of accumulated plant detritus.

ONCOIDAL TUFA FACIES

Oncoids form poorly cemented rudstones which display horizontal or cross bedding and in some cases normal grading. They occur as beds or lenses up to 1 m thick (see Fig. 11). Oncoids are common components of the tufa studied (Fig. 8A). They are well rounded and are mostly between 0.5 and 4 cm across. Their outer surface is smooth, in some cases even polished. Clasts of older tufa, predominantly of moss type, or phytoclasts – at present preserved as moulds, acted as oncoidal nuclei. The cortex is composed of alternating micritic and sparitic

Fig. 6. Stromatolitic tufa

A – stromatolite encrusting plant stems which are preserved as empty moulds, Háj; B – stromatolite composed of alternating porous and dense laminae, cross-section, Háj; C – dense and porous laminae seen under the microscope, algal filaments are visible, Háj; D – meandering larval housings, outer surface of stromatolitic lamina, Háj; E – cross-section of larval housings, each housing is covered with micritic lamina which grades upwards into sparry crystals, thin section, Háj; F–H – moulds of cyanobacterial or algal filaments composing stromatolites, filaments are covered with calcite crystals, SEM images, F – Hrhov, G, H – Háj



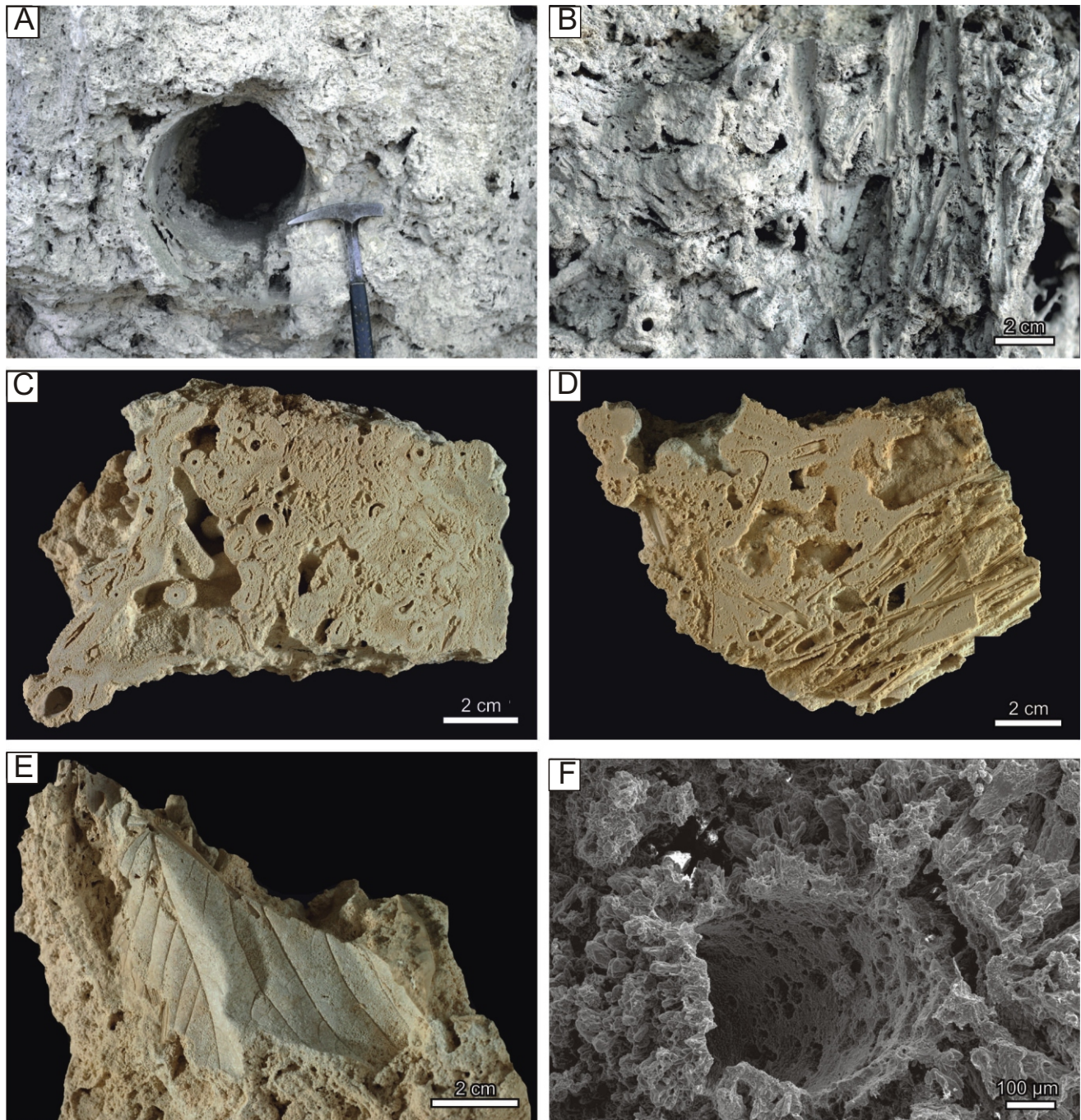


Fig. 7. Phytoclastic tufa

A – tree trunk mould, Hrhov, hammer head is 17 cm long; **B** – moulds of grasses in life position co-occurring within horizontally oriented twig moulds, Hrhov; **C** – twig moulds, cross-section, Hrhov; **D** – accumulation of encrusted leaves, Hrhov; **E** – leaf imprint, Hrhov; **F** – mould of small phytoclast entombed in calcite rim, the rim is composed of encrusted algal filaments, SEM image, Hrhov

laminae. It comprises moulds of cyanobacterial and algal filaments.

Interpretation. Oncoids commonly litter the beds of tufa-depositing streams (Pedley, 1990; Verrecchia et al., 1997). They form in active channels (Ordóñez and García del Cura, 1983; Vázquez-Urbez et al., 2013), which also seems to have been the case at the sites studied. Their cortex comprises algal and cyanobacterial moulds, which suggests that these microorganisms contributed to the accretion of the oncoids.

INTRACLASTIC TUFA FACIES

Intraclastic tufa comprises clasts derived from other tufa facies, namely moss, stromatolitic and phytoclastic facies as well as other grains, such as oncoids and peloids (Fig. 8B). Snail shells are an important component of this facies. Gravel- and sand-sized grains predominate. Fine-grained carbonate fractions occur subordinately. Charcoal grains were found occasionally. Intraclasts are poorly rounded and commonly coated with

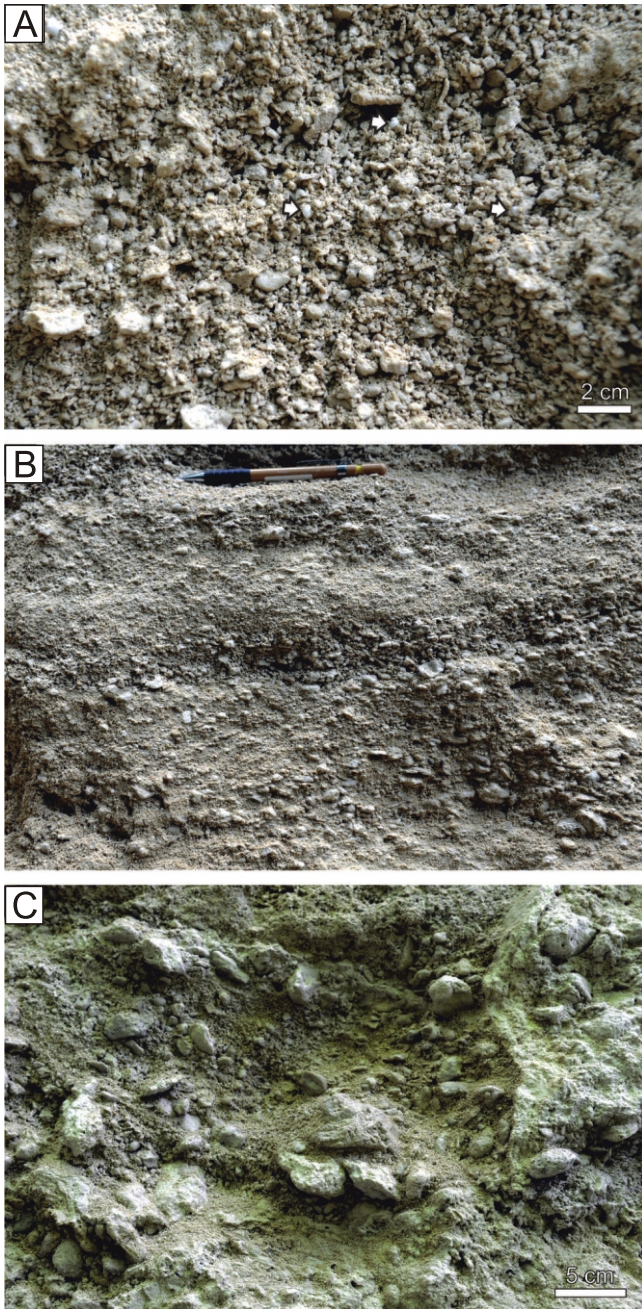


Fig. 8A – oncoloidal rudstone with snail shells (arrows), Háj; **B** – graded beds of intraclastic tufa with oncoids, the pen is 14 cm long, Háj; **C** – unsorted colluvial breccias composed of clasts of Triassic carbonate cemented with tufa, Háj

micritic rims. This facies build graded layers and lenses. The components are loosely cemented.

Interpretation. Intraclastic tufa is formed as a reworked product of the disintegration of older tufas of other types (e.g., Pedley et al., 2003). Coarse-grained clasts derived from resistant tufa facies whereas silt-sized components may have resulted from dismembering of calcite-encrusted algal filaments (e.g., Gradziński, 2010). Such deposits were laid down in flowing water, though in lower energy settings than all the other facies types described.

COLLUVIAL BRECCIAS

This facies occurs only locally in the uppermost part of some sections in the Háj Valley. It is composed of angular clasts of Triassic carbonates mostly a few centimetres across; however, the largest ones reach 40 cm across (Fig. 8C). The clasts are poorly sorted. Tufa clasts occur sporadically. Thin stromatolitic coatings cover and bind some clasts. The matrix is composed of tufa, chiefly of intraclastic type.

Interpretation. Immature Triassic debris derived from rock-craggs which occur on the valley slopes was gravitationally transported down and introduced into the tufa-depositing system. Bearing in mind the steep slopes of the valley, the debris is plausibly a rockfall or rockslide deposit (see Blikra and Nemeč, 1998).

FACIES ASSOCIATIONS

The facies distinguished are grouped into three facies associations that were formed in distinct environments, namely: dammed area, barrage and cascade facies associations. The first two are closely spatially linked.

CASCADE FACIES ASSOCIATION

This facies association crops out at the Hrhov and Gombasek sites (Fig. 9). It is composed predominantly of moss and phytoclastic tufas. Stromatolites are also common whereas intraclastic tufa facies occurs subordinately and oncoloidal tufa facies is absent. The dip of tufa layers averages between 10 to 30°, but in exceptional cases reaches 90°. The inclination partly results from that of pre-existing relief. The wood debris, such as tree trunks and branches, is oriented mainly sub-parallel to the strike of the tufa layers. It is only on steeper segments that they are oriented sub-parallel to the dip (see Gradziński, 2008). This facies association corresponds to the “cascade and barrage-cascade sequences” distinguished by Vázquez-Urbez et al. (2012) and the “cascade model” of Pedley (1990). It forms a single, extensive ramp-like structure, developed through progradation of tufa depositional lobes. The lobes did not act as a barrage and did not pond the water upstream. A lobe comprises several moss cushions which coalesced and prograded. Phytoclastic and intraclastic tufa were laid down predominantly in local depressions within a lobe, distributed in-between moss cushions.

BARRAGE FACIES ASSOCIATION

This association comprises the same facies as the cascade facies association. It also corresponds to the “cascade and barrage-cascade sequences” distinguished by Vázquez-Urbez et al. (2012). The main difference between cascade and barrage facies associations is the close spatial relationship between the latter and the dammed area facies association which is described below (Figs. 10 and 11). This relationship is clearly visible in the Háj Valley. Barrage facies association forms there several lithosomes up to 12 m in thickness. When the system was active these lithosomes acted as dams, which resulted in ponding of water in the upper segment of the stream. Seventeen inactive barrages were recognized in the Háj Valley. Some of these are narrow and have vertical faces whereas others are characterized by inclined, ramp-shaped downstream faces. The inclination of such a face varies between 30 and 50°.

Moulds of encrusted tree trunks and branches are an important component of this facies association. In the upstream part of

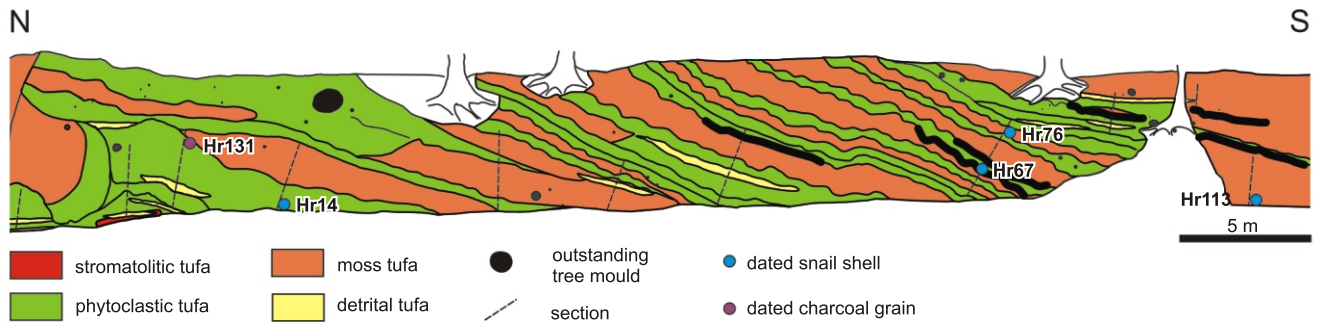


Fig. 9. Inclined beds of moss and phytoclastic tufa, which made up a tufa cascade

The location of samples for radiocarbon dating is indicated, Hrhov



Fig. 10. Spatial relationship between different tufa facies associations in the Háj Valley, vertically oriented layers of the barrage face (barrage facies association – BFA) are in contact with subhorizontally oriented layers of the inter-barrage facies association (IFA)

the barrage, they are placed horizontally and are oriented parallel to barrage elongation, that is more or less across the valley, whereas on steeply inclined downstream faces of a barrage, their orientation is parallel to the inclination of the face.

INTER-BARRAGE FACIES ASSOCIATION

Oncoidal and intraclastic tufa facies are the main components of this facies association (Fig. 11). Other facies contribute subordinately. This facies association is layered and poorly cemented, which results in its greater erodability in relation to cascade and barrage facies associations. This facies association bears some resemblance to “free flowing water channel-filling sequences” and “damming sequences” of Vázquez-Urbez et al. (2012). The mass occurrence of oncoids and gravel- to sand-sized lithoclasts corresponds to the former sequences, whereas its location between barrages is consistent with the latter. The relatively coarse-grained nature of the deposits, graded beds and cross-bedding all collectively suggest that the deposits in question were laid down in a flowing stream. It is similar to the “braided fluvial model” described by Pedley (1990).

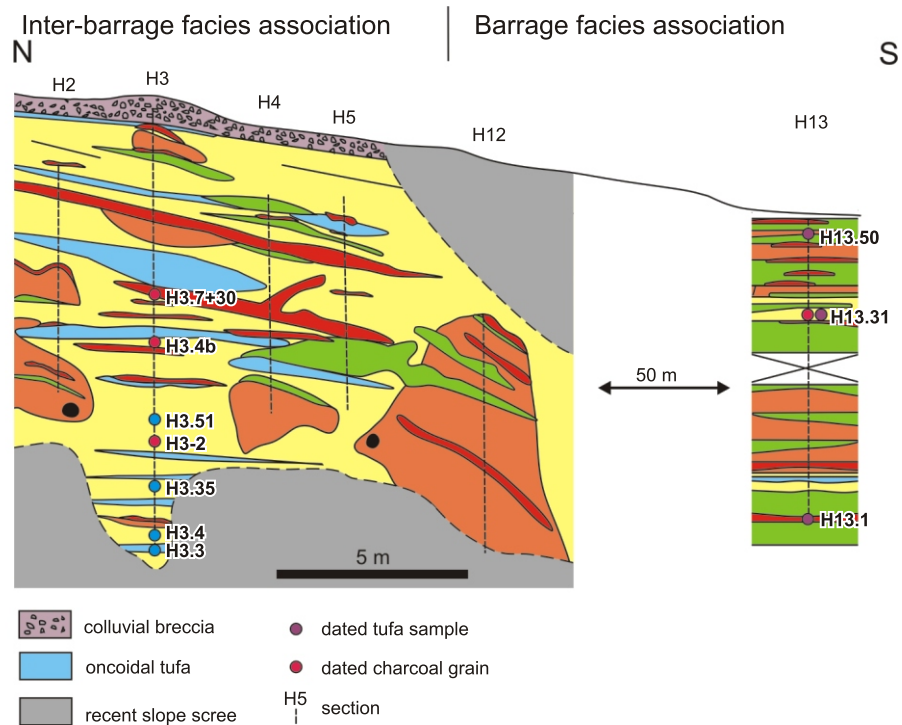


Fig. 11. Barrage and inter-barrage facies associations in the Háj Valley

The location of samples for radiocarbon dating is indicated; other explanations as in Figure 9

Table 1

Calcium carbonate content in the tufas studied

Site	Facies	<i>n</i>	CaCO ₃
Háj	mt	24	95.8
Háj	st	30	96.2
Háj	pt	16	95.2
Háj	ot	32	95.8
Háj	it	60	95.7
Háj	averaged	162	95.7
Hrhov	mt	66	96.6
Hrhov	st	1	96.9
Hrhov	pt	41	96.3
Hrhov	it	9	97.4
Hrhov	averaged	117	96.8
Gombasek	mt	17	91.0
Gombasek	pt	2	86.0
Gombasek	averaged	19	88.6

Data are given in wt.%; *n* – number of samples; it – intraclastic tufa, mt – moss tufa, ot – oncoidal tufa, pt – phytoclastic tufa, st – stromatolitic tufa

MINERAL AND CHEMICAL COMPOSITION OF THE FACIES STUDIED

The only autochthonous carbonate phase in all facies is calcite. Only some bioclasts – snail shells – are composed of aragonite. The tufas studied contain some admixtures of non-carbonate fraction. Their chemical composition is shown in Tables 1 and 2.

RADIOCARBON DATING

Radiocarbon dating of tufa is complicated by the lack of initial ¹⁴C activity. Due to carbonate depositional processes, initial ¹⁴C activity significantly differs from the activity of the active biosphere. Carbon in calcareous tufa consists of a mixture of old, inactive carbon from dissolved bedrock and biogenic carbon with ¹⁴C activity close to atmosphere activity. This causes differences between the actual sediment age and the conventional

age calculated under the assumption that the initial activity equals the activity of ¹⁴C in the biosphere. The difference, called the “apparent age” (“reservoir effect”), may range between 500 and 4500 years (Pazdur et al., 1988b).

To avoid this problem the organic matter incorporated within tufa was dated. However, the organic matter content in the sections studied is limited. Therefore, apart from some charcoal grains, shells of land snails were selected for radiocarbon dating. Although, even land snails can incorporate “dead carbon” into their shell (Goodfriend and Stipp, 1983), several studies have shown that land snail shells, especially of detritus feeders, provide reliable radiocarbon dates (e.g., Meyrick and Preece, 2001; Pigati et al., 2010). Radiocarbon dating results are shown in Table 3.

The tufa sections studied lack organic macrofossils. Only a few samples of charcoal were found, mostly from the middle part of the H3 section. Terrestrial snail shells were collected from the basal part of the H3 section and the HR section (Figs. 9 and 11).

Four samples of terrestrial snail shells from the Hrhov tufa were dated by the AMS technique (Table 3; Figs. 9 and 12). Based on calibrated age distributions, an age-depth model for the HR section was constructed using MOD-AGE software (Hercman and Pawlak, 2012). MOD-AGE takes into account full distribution of age as well as depth error estimation. Depth uncertainties for model construction were assumed at the level ± 10 cm (assuming normal distribution). The chronology obtained (age-depth model) is shown in Figure 12. Based on the chronology obtained, the period of section HR deposition may be estimated at between ca. 3500 and 6300 cal. years BP (samples Hr14, Hr67, Hr76, Hr113; Fig. 9). Apart from snail shells, one charcoal grain (sample Hr131) was dated from this section. However, it provided an unexpectedly old date of 42,950–40,150 cal. years BP, incompatible with the other ¹⁴C dates as well as with snail and plant fossils from this tufa (see Němejc, 1936, 1944; Petrbock, 1937; Ložek, 1955). Thus, the most probable explanation is redeposition of an old charcoal grain and its incorporation into growing tufa. Charcoal is quite inert and can be easily transported (Scott, 2010 and reference therein). The redeposition of charcoal is a common feature in a lake environment (e.g., Wittlock and Millspeugh, 1996; Walker, 2007); however, to the best of the authors' knowledge, it has not been recognized in a tufa depositional environment so far.

Section H13 was devoid of useful material for radiocarbon dating except for one sample of charcoal from the 200 cm depth (sample H13.31; Fig. 11). The age of this charcoal was 4830–4570 cal. years BP (95.4% probability). Three carbonate samples of tufa were additionally dated (samples H13.1,

Table 2

Chemical composition of the tufas studied

Site	Facies	<i>n</i>	SiO ₂	Al ₂ O ₃	Fe ₂ O ₃	Na ₂ O	K ₂ O	TiO ₂
Háj	mt	1	0.40	0.10	0.02	0.01	0.02	0.01
Háj	st	3	0.40	0.10	0.10	0.02	0.02	0.01
Háj	pt	2	0.34	0.08	0.04	0.01	0.01	0.01
Háj	ot	9	0.60	0.13	0.08	0.02	0.03	0.01
Háj	dt	14	1.04	0.22	0.15	0.04	0.04	0.02
Háj	averaged	29	0.77	0.17	0.12	0.03	0.03	0.02
Hrhov	mt	19	0.79	0.22	0.10	0.04	0.04	0.01
Hrhov	pt	11	0.78	0.23	0.11	0.05	0.04	0.01
Hrhov	averaged	30	0.79	0.23	0.12	0.06	0.04	0.02
Gombasek	mt	2	4.75	1.83	1.12	0.04	0.33	0.07

Data are given in wt.%; dt – detrital tufa; other explanation as in Table 1

Table 3

Radiocarbon dating results

Sample	Laboratory number	Sample type	Radiocarbon age [yr BP]	68.2% conf. interval		95.4% conf. interval	
				Cal. age range [yr BP]	Prob. [%]	Cal. age range [yr BP]	Prob. [%]
H13.31	Poz-50420	ch	4160 ± 35	4830–4780 4770–4620	12.2 56.0	4830–4570	95.4
H13.31	MKL-1824	c	8580 ± 80				
H13.1	MKL-1826	c	6210 ± 90				
H13.50	MKL-1828	c	5040 ± 60				
H3-2	Poz-50417	ch	6320 ± 50	7310–7170	68.2	7420–7350 7340–7160	7.1 88.3
H3.4b	Poz-50418	ch	6250 ± 35	7250–7160	68.2	7270–7150 7120–7020	78.5 16.9
H3.7+30	Poz-50419	ch	6110 ± 40	7160–7120 7020–6900	11.1 57.1	7160–6890	95.4
H3.3	Poz-53536	s, Ch.f.	6195 ± 35	7170–7150 7130–7020	7.1 61.1	7250–7190 7180–6990	5.1 90.3
H3.4	Poz-53537	s, Ch.f.	6070 ± 35	6985–6885	68.2	7150–7120 7020–6830 6820–6790	2.0 89.3 4.1
H.3.51	Poz-53538	s, Ch.f.	6195 ± 35	7170–7150 7130–7020	7.1 61.1	7250–7190 7180–6990	5.1 90.3
H3.35	Poz-53539	s, Ch.f.	6105 ± 35	7150–7120 7020–6910	6.9 61.3	7160–6880	95.4
HR131	Poz-50422	ch	36800 ± 800	42,350–41,050	68.2	42,950–40,150	95.4
HR 14	Poz-53540	s, O.e.	5350 ± 35	6270–6250 6210–6170 6160–6110 6080–6020	3.6 17.4 22.6 24.6	6280–6230 6220–6000	9.6 85.8
HR 67	Poz-53541	s, C.i.	4680 ± 70	5580–5550 5480–5310	5.7 62.5	5590–5280	95.4
HR 76	Poz-53542	s, C.v	4105 ± 35	4800–4760 4690–4670 4650–4520	16.3 4.1 47.8	4820–4750 4730–4520 4470–4450	22.6 71.6 1.3
HR 113	Poz-53544	s, O.g.	3780 ± 40	4240–4080	68.2	4300–4070 4050–3990	87.4 8.0

Poz – Poznań Radiocarbon Laboratory (Poland), MKL – Laboratorium Datowań Bezwzględnych (Absolute Dating Laboratory, Skala, Poland); c – calcareous tufa, ch – charcoal, s – snail shell, Ch.f – *Chilostoma faustinum*, C.i. – Clausilidae indet., C.v. – *Cepae vindobonensis*, O.e. – *Oxyloma elegans*, O.g. – *Oxychillus glaber*

H13.31, H13.50; Fig. 11). Conventional ages of carbonate samples were not consistent with the stratigraphical order (Table 3). One of the samples dated was collected from the depth of 200 cm, that is the same as the dated charcoal grain. Comparison of ^{14}C ages of both samples should enable the estimation of the apparent age of the tufa sample. However, the attempt of apparent age estimation was completely unsuccessful. Assuming an apparent age of 5550 ± 115 years, as suggested by the difference between the radiocarbon ages of charcoal and carbonate samples, the corrected ages of other carbonate samples were completely impossible. For example, the uppermost sample gives a corrected age of -490 ± 175 years.

Three explanations are possible. They are as follows: (1) the apparent age of the tufa sample from the depth of 200 cm was correct, while the other samples suggest strong changes of apparent age in the course of tufa deposition; (2) carbonate samples from bottom and top layers are rejuvenated by incorporation of younger calcite cement in pore space; and (3) the charcoal

fragment was redeposited and was older than the host tufa. The last explanation does not account for the inconsistent stratigraphic order of the tufa dates in the H13 section.

Charcoal fragments and terrestrial snail shells from the H3 section were dated. Four samples of terrestrial snail shells were collected from the bottom part of the H3 section (samples H3.3, H3.4, H3.35, H3.51) whereas the charcoal samples were derived from the bottom and middle parts of the section (samples H3-2, H3.7+30, H3.4b; Fig. 11).

Based on calibrated radiocarbon age distributions, an age-depth model for the H3 section was constructed using MOD-AGE software (Hercman and Pawlak, 2012). MOD-AGE takes into account full distribution of age as well as depth error estimation. Depth uncertainties for model construction were assumed at the level ± 10 cm (assuming normal distribution). The chronology obtained of the H3 section (age~depth model) is shown in Figure 13. Based on the chronology obtained, deposition of the H3 section took place between ca. 7400 and 6300 cal.

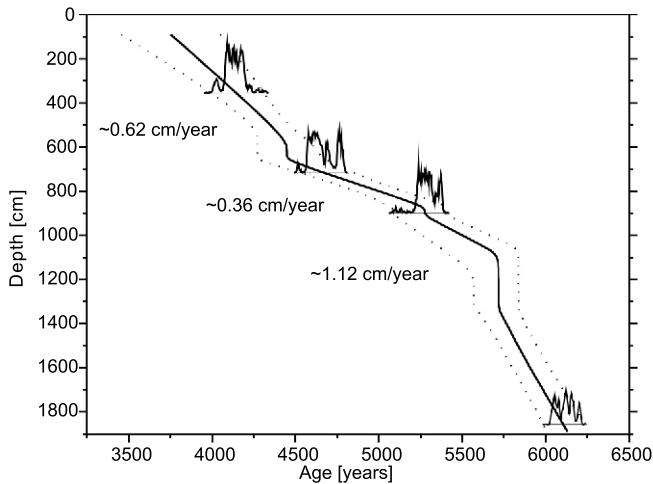


Fig. 12. Age-depth model for the Hrhov section

Thick line – relation of age and depth; dotted line – 2 sd confidence band for estimated relation; radiocarbon age probability distributions located at the sampling depth; mean tufa growth rate between dated layers are marked

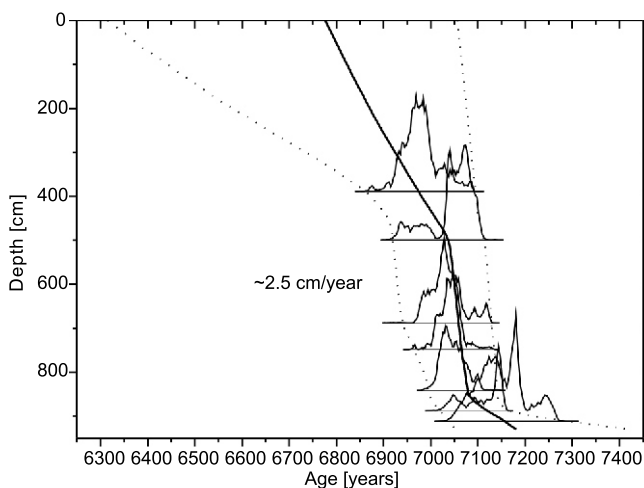


Fig. 13. Age-depth model for snail shells and charcoal grains dated from the Háj (H3 section)

Explanations as in Figure 12

years BP. However, this is based on the assumption of a constant growth rate of tufa, which was probably not the case.

DISCUSSION

DEPOSITIONAL SYSTEMS

Two depositional systems were recognized within the tufas studied. The tufas at Hrhov and Gombasek represent a perched springline transverse system whereas the tufas in the Háj Valley correspond to a longitudinal fluvial system.

FLUVIAL DEPOSITIONAL SYSTEM

There is much resemblance between the tufas at Háj and fluvial tufa systems described worldwide (e.g., Golubić, 1969; Pedley, 1987, 1990, 1993; Pedley et al., 1996; Pentecost, 2005;

Arenas-Abad et al., 2010; Vázquez-Urbez et al., 2012). Tufas at Háj include two facies associations, namely the barrage and dammed area facies associations (Figs. 10, 11, 14 and 15). The barrages at Háj, as in the other systems, caused ponding of water in the upstream section of the valley and hence created accommodation space for oncoidal and detrital tufa facies.

Pedley et al. (1996) concluded that barrage shape and size depend upon climatic conditions. Wide barrages, with inclined downstream faces composed of buttresses formed by mosses or liverworts, are typical of temperate-climate fluvial tufa systems. This was documented in extinct Holocene systems in Caerwys and Alport, in the United Kingdom (Pedley, 1987, 1993). Upstream faces of barrages are vertical there, and in upstream ponded segments of the streams fine-grained tufa of mudstone or wackestone was deposited. Conversely, in a Mediterranean climate narrow barrages with vertical faces are developed (Pedley et al., 1996). Deeper lakes exist between barrages. The most spectacular modern examples of such systems are the Plitvice Lakes (Emeis et al., 1987) and the Ruidera Lakes (Pedley et al., 1996; Ordóñez et al., 2005). This pattern results from faster vertical growth of tufa barrages stimulated by warm, semi-arid climatic conditions, whereas in a temperate climate lateral growth of barrages equals their vertical growth (Pedley et al., 1996). The fluvial system in the Háj Valley comprises various types of barrage (Figs. 11 and 14). Some have vertical downstream faces whereas in others this face is inclined (Figs. 5B and 10). Thus, the geometry of barrages seems also to be controlled by factors other than climate. A similar notion was presented by Viles and Pentecost (2007) as well as by Vázquez-Urbez et al. (2012). The barrages in the Háj Valley developed in narrow places, where the valley was constricted by rocky ridges on its slopes, or in irregularities in the pre-existing valley bottom. The inception and growth of barrages, especially of the former location, was facilitated by wood debris jams. The Háj Valley tufa system shares the above characteristics with other tufa systems (e.g., Florsheim et al., 2013).

Relatively coarse-grained oncoidal and intraclastic tufa facies were deposited between barrages, suggesting a high-energy depositional milieu, which distinguishes Háj from other barrage fluvial tufa systems (Figs. 8A, B and 11). For example, in Caerwys, lime mudstone and wackestone were laid down upstream of barrages (Pedley, 1987). Similarly, in dammed areas of the closely studied Piedra, Mesa and Añamaza rivers fine grained tufa was deposited (Vázquez-Urbez et al., 2012; Arenas et al., 2013). This difference suggests that lakes were not created in the dammed areas at Háj; conversely, there existed active stream channels. Thus, this implies that although the aggradation of inter-barrage areas was not so high as that of barrages, it was not substantially slower. The spatial relationship of a dammed area facies association with a small, secondary barrage suggests that the minimal depth of inter-barrage areas was around 0.5 m (Fig. 11). A similar conclusion comes from the section published by Ložek (1958: table III 1, 2, table VI), which depicts tufa in a lower segment of the Háj Valley. This segment is presently poorly exposed. Such a depth enabled long-lasting high-energy conditions in the stream sections located upstream of the barrages.

The spatial relationship of barrages and inter-barrage deposits, which was reconstructed for the upper segment of the Háj Valley, points to different vertical growth rates of the barrages (Fig. 14). The lowermost barrage is the highest one. Its top reaches the level of the accumulation terrace. Several barrages located upstream do not reach this level. Rather, they are covered by deposits of inter-barrage facies association. Thus, the lowermost located barrage aggraded with the highest rate which resulted in drowning of all of the smaller barrages up-

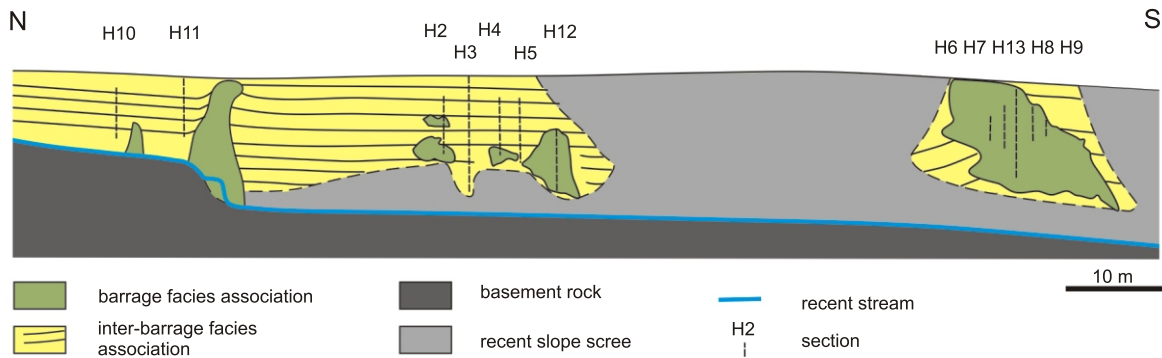


Fig. 14. Distribution of former barrages and inter-barrage areas in the upper segment of the Háj Valley

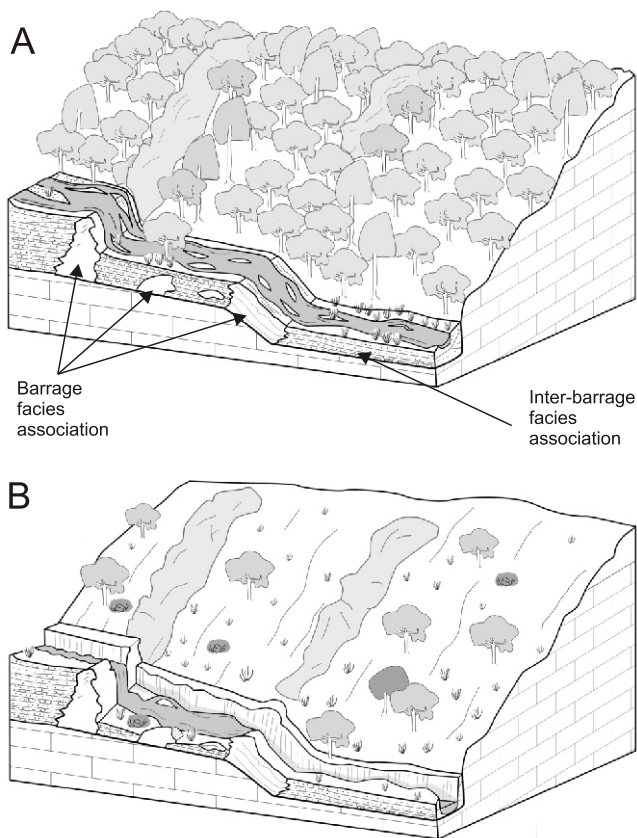


Fig. 15A – model of sedimentation; B – erosion of the longitudinal fluvial tufa system developed in narrow valleys, for instance in the Háj Valley

stream. They finally were buried by oncolidal and intraclastic tufa facies. A similar mechanism was described by Golubić (1969); however, in his example inter-barrage areas were flooded, which caused cessation of secondary barrage growth (see also Pedley, 1990).

PERCHED SPRINGLINE DEPOSITIONAL SYSTEM

The tufa studied at Hrhov clearly corresponds to the “perched springline model” defined by Pedley (1990), Ford and Pedley (1996) and Pedley et al. (2003) or the “slope travertine system” distinguished by Violante et al. (1994). The tufa was fed by a perched spring on the side of the valley, the location of which resulted from the occurrence of impermeable Lower Triassic clastic strata (Figs. 2–4). The steep slope below the spring

prevented the creation of barrages and extensive dammed areas and caused formation of a lobe-shaped tufa body (Fig. 16). A similar relationship was noted in fluvial tufa in Spain, where the size of dammed areas clearly depended upon the inclination of the river bed (Vázquez-Urbez et al., 2012). Additionally, the moderately steep slope enabled the creation of a new outflow zone, in the case of damming. This led to the formation of a new depositional lobe, which finally coalesced with the previously active one as a consequence of tufa growth.

Many tufas of perched springline type have limited areas (Pedley et al., 2003). The exceptions include the Matlock Bath deposits (Derbyshire, UK) with an area of about 6 ha (Pentecost, 1999) and Rocchetta a Volturno (southern Italy) with an area of around 10 km² (Violante et al., 1994). Therefore, the tufa at Hrhov with its aerial extent around 17.5 ha (Kilić, 2008) is among the most extensive recognized so far.

The poorly exposed tufa at Gombasek also represents a perched springline transverse depositional system. Tufa was laid down on a gently inclined slope, adjacent to a low-lying river terrace. These features enable discrimination between Gombasek and Hrhov and other thus-far described springline tufas (see for instance Pedley, 1990; Violante et al., 1994; Pentecost, 1999; Pedley et al., 2003; Vázquez-Urbez et al., 2012). However, the Gombasek tufa shares several similarities with them, as for instance deposition near a resurgence, the point-source supply of water, domination by moss tufa facies (Figs. 3C and 5A). The main factor which influenced such a development of tufa at Gombasek was most probably the general topography, that is, the wide mouth of the lateral, dry valley to the alluvial plain of the main river. The facility of lateral migration of flow prevented the water from being ponded and thus impeded the formation of a typical fluvial system comprising barrages and dammed areas. Conversely, such unconfined conditions favour the creation of lobate morphology typical of springline tufas and the development of a fan-shaped tufa body.

Neither of the sites described above contain moss tufa curtains which are a typical component of perched springline tufas. This resulted from deposition of the tufa studied on moderately steep or gently slopes in the case of Hrhov and Gombasek, respectively. Conversely, most of the tufas described so far of this type were laid down on steep slopes with some vertical sections, which promoted the formation of tufa curtains (e.g., Pedley et al., 2003; Vázquez-Urbez et al., 2012).

There is an abundance of phytoclastic tufa facies at Hrhov. This facies type is not common in perched springline tufas that are typically dominated by moss and stromatolitic facies (Pedley, 1990; Pentecost, 1999; Pedley et al., 2003), whereas it is a typical component of a longitudinal, stepped fluvial tufa system (Pedley, 1990; Ford and Pedley, 1996; Arenas-Abad et al., 2010; Vázquez-Urbez et al., 2012). The formation of this facies clearly depends upon stream capacity. At present, the resurgence at Hrhov expels a very large amount of water. Its maximal

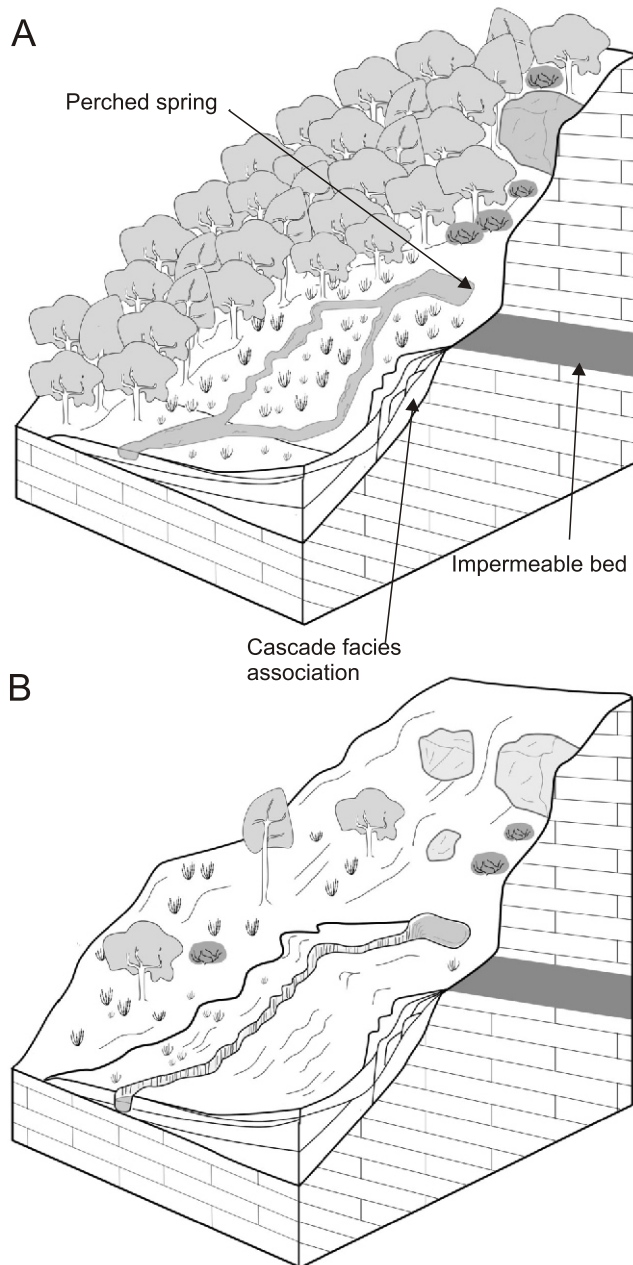


Fig. 16A – model of sedimentation; B – erosion of transverse perched springline tufa developed on plateau slopes, for instance at Hrhov and Gombasek

discharge is estimated at 740 l/s (Jakál and Bella, 2008). Thus, based on present-day data, one may infer that a stream feeding the tufa studied carried enough water to easily transport plant detritus. Conversely, many other springline tufa systems are fed by a small amount of water, which impedes transport of a significant amount of plant detritus. For example, the total discharge of all springs located near the extensive springline tufas at Matlock Bath does not exceed 60 l/s (Pentecost, 1999). A second key factor contributing to the deposition of phytoclastic facies is the presence of vegetated areas which could provide plant debris into the tufa depositional system. At Hrhov the area between the resurgence and the tufa outcrop studied is clearly more extensive than it is at Gombasek (Fig. 3). This is in line with the com-

mon occurrence of phytoclastic facies at the former site and its scarcity at the latter one.

FACTORS INFLUENCING THE GEOCHEMICAL COMPOSITION OF TUFA

The geochemical composition of tufa varies among the particular facies and among the particular sites studied (Tables 1 and 2). The enrichment of tufa in Si, Al, Fe and Ti is a proxy for non-carbonate detrital impurities in the water (Sürmelihindli et al., 2013). Microbial biofilms covering the surface of growing tufa are especially prone to capturing such detrital impurities (Pedley, 1992; Gradziński et al., 2010). The differences among particular sites reflect various palaeohydrological conditions persisting during tufa growth. Taking into account the uniform age of the tufas studied, local conditions seem to be responsible for these differences.

A lower calcium carbonate content and a higher content of elements, such as Si, Al, Fe, Na, K and Ti, characterise the tufa from Gombasek (Tables 2 and 3). This resulted from the occurrence of Lower Triassic shales and marlstones in the catchment, even in close proximity to the tufa (Fig. 2; Mello, 1996). Moreover, the karst hydrological system feeding the spring at Gombasek drains also some areas of plateau where the above-mentioned Lower Triassic rocks crop out (Bella, 2003; Haviarová et al., 2012 and references quoted therein). Thus, non-carbonate admixtures were most probably transported also via an underground drainage system. The substantial accumulation of fine-grained clastic deposits in Gombasecká Cave supports the above view.

A higher calcium carbonate content and the smallest amount of Si, Al, Fe and Ti characterize the tufas from the Háj and Hrhov sites, though the geological settings of these sites differ considerably. Non-carbonate rocks, such as phyllites and metabasic rocks, crop out in the upper part of the catchment of the Háj Valley (Fig. 2; Mello, 1996). Conversely, the catchment of the spring feeding the Hrhov tufa is composed exclusively of carbonate rocks. Thus, the elevated content of non-carbonate admixtures in this tufa can be explained in a twofold way. It may be the result of the concentration of residua after limestone dissolution. A mechanism similar to that operating at Gombasek could also be taken into consideration. The underground flow may be in contact with Lower Triassic shales and marlstones and hence may transport some fine-grained siliciclastic material. The location of the spring near the contact of Middle Triassic carbonates and underlying clastic rocks supports such a scenario. Thus, the presence of non-carbonate admixtures manifested by elevated contents of such elements as Si, Al, Ti incorporated within tufa is a good indicator of catchment geology and sources of the water that fed the tufa. For instance, Holocene tufa sequences in the Polish Uplands abound in marly and muddy horizons with fine-grained siliciclastic material (Szulc, 1984; Pazdur et al., 1988a; Alexandrowicz, 2004). This originated as redeposited Pleistocene loess-covers which are widespread in that region and are easily erodable (see Bíl and Kubeček, 2012).

Differences in chemical composition between particular facies are also visible (Tables 1 and 2). The most pronounced feature is the lowest calcium carbonate content and the highest content of Si, Al, Fe and Ti in intraclastic tufa facies in the Háj Valley. This indicates that the inter-barrage areas acted as effective traps for detrital components derived from the upper part of the catchment. In other tufa systems, inter-barrage facies comprise marl (Vázquez-Urbez et al., 2012; Arenas et al., 2013), clayey tufa or even clay (Pedley, 1993).

HISTORY OF HOLOCENE TUFA IN THE SLOVAK KARST:
 ITS RISE, FALL AND REBIRTH

The contact between basement rocks and tufa was not found in the course of this study. Thus, the beginning of the tufa growth cannot be analysed either in terms of environmental conditions or in terms of time. The earliest studies by Němejc (1936), Petrbok (1937) and Ložek (1955, 1958) do not mention the inception of the tufa-depositing system. The dates obtained clearly show that the system was fully operating in Mid Holocene time, that is during the Atlantic and Sub-Boreal intervals (ca. 7.5–3.5 ka BP; Figs. 15A and 16A). Thus, the tufa achieved its acme of growth then. Bearing in mind the dating results, the growth rate of tufa may be estimated at between 0.36 and 1.12 cm per year at Hrhov and at around 2.5 cm per year at Háj during Atlantic time (Figs. 12 and 13). This is considerably higher than the growth rate of other Holocene tufas in Europe. For instance, Meyrick and Preece (2001) calculated the growth rate of Atlantic (ca. 7.9–7.2 ka old) tufa from Courteenhall, English Midlands, as 0.7 mm per year. However, that tufa is clay-rich and probably represents paludal facies, thus one can expect a considerably lower growth rate. Higher values, reaching 6.3 mm per year, were calculated by Limondin-Lozouet and Preece (2004) for ca. 5.3–4.5 ka old tufa in Normandy. Pazdur et al. (1988b) obtained the rate of growth of stromatolitic tufa ca. 3–1.2 k.a. old in the Raclawka Valley (southern Poland) at up to 10 mm per year. However, measurements of recent barrage tufa in north Australia gave maximal values of up to 32.22 mm per year, whereas mean values equal 4.15 mm per year (Drysdale and Gillieson, 1997). Weijermars et al. (1986) reported even higher values, reaching 140 mm per year, from extinct Quaternary moss tufa in Spain.

During the tufa growth in the Atlantic period the area studied was forested, as inferred from the associated mollusc (Figs. 15A and 16A; Kormos, 1912; Petrbok, 1937; Ložek, 1955, 1958) and plant fossils (Figs. 6A and 7; Nemejc, 1936, 1944). Steep slopes of the valley did not provide significant amounts of rock debris into the growing tufa. This probably resulted from stabilization of the slopes by a dense vegetation cover (Viles et al., 2008).

A very characteristic feature of the tufa at Háj and Gombasek is the incision of streams down to 6 and 12 m at the former and latter sites respectively (Figs. 15B and 16B). The incision shows that the tufa experienced cessation of growth and substantial erosion. The present relief of the Háj Valley is clearly dependant upon the distribution of facies associations of inactive, eroded tufa. The relatively hard and resistant barrage facies association forms jumps and constrictions in the longitudinal profile of the valley whereas wider valley segments are carved in dammed area facies associations (Figs. 3A, 4B, 14 and 15B). Tufa at Hrhov most probably was eroded too, but the incision was later obliterated by quarrying. Thus, the sites studied recorded the same phenomenon as is clearly visible all over Europe, since many European tufas show arrested growth in the Late Holocene (Goudie et al., 1993). Subsequent studies showed this phenomenon in other European tufa sites (e.g., Preece and Day, 1994; Preece and Bridgland, 1999; Gradziński et al., 2001; Soligo et al., 2002; Žák et al., 2002; Meyrick, 2003; Limondin-Lozouet and Preece, 2004; Alexandrowicz, 2004, 2012; Capezzuoli et al., 2010) as well as on other continents (Pentecost and Zhang, 2001; Carthew and Drysdale, 2003; Turner and Jones, 2005; Moyersons et al., 2006).

The dating results obtained in this study do not shed new light on the cessation time, because of serious problems with precise dating of the tufa. However, the tufa must have stopped growing later than 4830–4570 cal. years BP and 4300–3990 cal.

years BP, since these are the ages of the youngest dated charcoal grain from the tufa sections at Háj and youngest dated snail shell at Hrhov (Table 3), respectively. Ložek (1955, 1958) found artefacts younger than Neolithic in the upper part of the tufa sections in the lower segment of the Háj Valley and at Hrhov. The Slovak Karst area is considered to have been extensively inhabited in the Late Bronze Age and Early Iron Age, that is between 1100 and 450 BC (Bánesz, 1994; Soják, 2008). Thus, the incision most probably commenced during or just after this time span. Despite the dating uncertainties, the tufas clearly ceased to grow in late Sub-Boreal or around the boundary of the Sub-Boreal and Sub-Atlantic (i.e., ca. 2.5 ka BP).

Goudie et al. (1993) listed and discussed 26 factors that may have been responsible for the Late Holocene decline in the deposition of tufa. They concluded that this phenomenon may have been a compound effect caused by overlap of several factors, notably anthropogenic pressure and climatic changes.

It seems to be impossible to show unequivocally which factor caused cessation of growth of the tufa studied. Nonetheless, three scenarios can be formulated: (1) the chemical parameters allowing precipitation of tufa did not change, incision being caused solely by increasing erosive capacity of the streams, (2) the erosive capacity of streams remained constant but changes in the chemical composition of the water impeded tufa growth, which resulted in erosion of earlier-deposited tufa, and (3) erosion was caused by the cumulative effect of changing chemical parameters of the water and increasing erosive capacity of the streams.

Colluvial deposits covering the tufas in the Háj Valley suggest that pronounced redeposition from the slopes commenced during and continued after tufa sedimentation (Figs. 8C and 10). Similar deposits have been found in the upper part of tufa sections in the lower segment of the Háj Valley (Ložek, 1958). However, local introduction of colluvium into a tufa-depositing system does not seem to be a factor significantly impeding tufa growth. Conversely, deposition of isolated colluvial lobes in the tufa-depositing stream should stimulate the development of new tufa barrages (Florsheim et al., 2013) and, therefore, should enhance tufa deposition. On the other hand, increasing colluvial activity resulted also in introducing fine-grained clastic material from the slopes into the tufa-depositing systems. In a fast-flowing stream the fine-grained clastic particles were easily put in motion and became transported sediment load. Therefore, they may have impacted the growing tufa by mechanical abrasion. They may also have greatly affected the microbial biofilms essential for tufa growth (Pedley, 1992; Gradziński, 2010).

The slope instability implied as a cause of redeposition from the slopes is often caused by forest retreat; hence it seems plausible that the area experienced such a process (Figs. 15B and 16B). This is supported by the pollen data obtained from a local peat-bog where the pollen spectra record an important amount of non-arboreal pollen in Pre-Boreal peat (Krippel, 1957). The retreat of forest is also clearly recorded within mollusc assemblages in the Hrhov and Háj tufas (Ložek, 1955, 1958). Humid conditions were another factor which, along with retreat of forests, affected slope stability. The pollen spectra from the peat-bog registered some humid conditions at the beginning of the Sub-Atlantic, that is plausibly during tufa erosion (Krippel, 1957).

Deforestation also causes increased soil erosion (e.g., Ford and Williams, 2007: p. 473–477), which greatly reduces the capacity to dissolve calcium carbonate in an epikarst zone. Experimental work carried out by Zambo and Ford (1997) in the Hungarian part of the same karst area where the tufa sites studied are located, demonstrated that the capacity to dissolve calcium carbonate is relatively low beneath thin soil cover. This has an

effect on the amount of dissolved calcium carbonate in ground and spring water (Goudie et al., 1993). Steidtmann (1936) noted that the calcium carbonate content in springs draining unbroken forests in Lexington (Virginia, USA) was three times greater than in springs draining pastoral areas. Low calcium carbonate content in spring water lowers the possibility of calcium carbonate precipitation in the form of tufa. Therefore, one can hypothesize that deforestation impacted the tufa depositional system in at least a twofold way, via increase in the erosive capacity of streams, and via decrease in the dissolved calcium carbonate content of the stream water.

The above scenario supports the theory that prehistoric humans influenced the cessation of tufa growth since they were responsible for deforestation, which in turn created conditions triggering the disintegration of tufa. It seems plausible that the forest retreat in Slovak Karst reflected growing pastoral or agricultural activity of prehistoric humans (Ložek and Prošek, 1956). Coincidence with establishment of the Kyjatice or Hallstatt culture in the area studied supports this view. Artefacts from these cultures have been found not only in tufas (Ložek, 1955, 1958) but also in numerous caves, including those in close proximity to the tufa sites studied (Bánesz, 1994; Bárta, 1994; Soják, 2007, 2008). However, deforestation might also have been completely independent of prehistoric human activity. It may have been driven solely by climatic factors, mainly aridification and warming. In such a view, the coincidence of human settlement and cessation of tufa growth may be purely accidental.

Whatever the factors that stimulated disintegration of tufa and incision of streams, they ceased to operate, as modern tufa are growing at all the sites studied (Fig. 4B; Němejce, 1936; Kovanda, 1971; Kilík, 2008). In the Háj Valley, in the place of old, inactive barriers constructed of moss and stromatolite tufa, recent tufa representing the same facies types are being developed. They form spectacular curtains constantly flushed with water (Fig. 4B; Gradziński, 2010). Similar curtains are forming at Hrhov. At Gombasek the modern stream is confined to a gully entrenched into an old tufa fan. This results in the formation of modern tufa in the limited space of the bottom part of this narrow gully. Tufa forms barrages and is being deposited in inter-barrage areas composed of stromatolite tufa and oncoidal tufa, respectively. The recent tufa represents a longitudinal fluvial depositional system, and so it differs from its Holocene counterpart which was a perched springline type. The varying ability of lateral migration of a stream seem to be one of the most important differences between the two depositional systems. Thus, the Slovak Karst represents an example of an area where after a late Holocene decline, tufa deposition was reactivated and has been persisting in a manner similar to that in some British and Czech areas (Baker and Simms, 1998; Žák et al., 2002). The causes of this process have not been identified.

CONCLUSIONS

1. Tufa in the Slovak Karst area represents longitudinal fluvial and transverse perched springline depositional systems.
2. The fluvial depositional system comprises tufa forming barrages and filling inter-barrage areas. The former are composed of moss, stromatolitic and phytoclastic tufa facies, whereas the latter comprise chiefly oncoidal and intraclastic tufa facies. Fluvial tufas were laid down in narrow, steep-sided valleys down which a confined stream flowed with limited lateral migration. Barrages were formed in constrictions of a valley or associated with irregularities in the pre-existing valley bottom. Wood debris jams enabled inception and growth of barrages. In the inter-barrage areas, active stream channels existed, where oncoidal and intraclastic tufa was laid down.
3. Perched springline tufas were deposited below resurgences located on the plateau slopes. Steep slopes prevented the creation of barrages and extensive dammed areas. This resulted in the formation of a lobe-shaped tufa body. Such tufas comprise moss, stromatolitic and phytoclastic tufa facies.
4. The amount of non-carbonate admixtures in the tufa studied strongly depends upon the lithologies present in the surface catchment area and probably also in the karst-draining system which feeds the tufa.
5. The tufas studied were formed in the Mid-Holocene, namely in Atlantic and Sub-Boreal times. Subsequently, they experienced substantial erosion and were incised down to their Mesozoic basement. Erosion is hypothesized to have been stimulated by deforestation caused by prehistoric humans.
6. Following erosion, this deposition of tufa was renewed. At present tufa grows at all the sites studied.

Acknowledgements. The study was financed by the National Science Centre grant N N307 151538. The study was realized in the frame of collaboration between the Institute of Geological Sciences, Jagiellonian University, and the Slovak Museum of Nature Protection and Speleology. The authorities of the Krajský Úrad Životného Prostredia in Košice and the Národný Park Slovenský Kras gave permissions for field-work. M. Jasionowski (Warsaw, Poland) and P. Holúbek (Liptovský Mikuláš, Slovakia) made literature accessible to the authors. R. Gradziński, R. Jach and A. Kargól assisted in the field. M. Orvošová, P. Bella, as well as M. and M. Terray kindly provided logistic support during the field-work. E. Stworzewicz determined fossil snails, B. Zych operated the SEM, R. Jach and P. Szelerewicz patiently prepared some of the figures. The authors acknowledge all these individuals and institutions. The paper greatly benefited from constructive reviews by C. Arenas-Abad and P. Bella and from corrections by the editors T. Peryt and J. Zalasiewicz to whom the authors are greatly indebted.

REFERENCES

- Alexandrowicz W.P. (2004) Molluscan assemblages of Late Glacial and Holocene calcareous tufas in southern Poland. *Folia Quaternaria*, **75**: 3–309.
- Alexandrowicz W.P. (2012) Assemblages of molluscs from Sulislawice (Małopolska Upland, southern Poland) and their significance for interpretation of depositional conditions of calcareous tufas in small water bodies. *Annales Societatis Geologorum Poloniae*, **82**: 161–176.
- Andrews J.E. (2006) Palaeoclimatic record from stable isotopes in riverine tufas: synthesis and review. *Earth-Science Reviews*, **75**: 85–104.
- Andrews J.E., Brasier A.T. (2005) Seasonal records of climatic change in annually laminated tufas: short review and future prospects. *Journal of Quaternary Science*, **20**: 411–421.
- Anzalone E., Ferreri V., Sprovieri M., D'Argenio B. (2007) Travertines as hydrologic archives: the case of the

- Pontecagnano deposits (southern Italy). *Advances in Water Resources*, **30**: 2159–2175.
- Arenas C., Vázquez-Urbez M., Auqué L., Sancho C., Osácar C., Pardo G.** (2013) Sedimentology and depositional architecture of tufas deposited in stepped fluvial systems of changing slope: lessons from the Quaternary Añamaza valley (Iberian Range, Spain). *Sedimentology*, **61** (in press) doi: 10.1111/sed.12053.
- Arenas-Abad C., Vázquez-Urbez M., Pardo-Tirapu G., Sancho-Marcén C.** (2010) Fluvial and associated carbonate deposits. *Developments in Sedimentology*, **61**: 133–175.
- Baker A., Simms M.J.** (1998) Active deposition of calcareous tufa in Wessex, UK, and its implications for the “late-Holocene tufa decline”. *Holocene*, **8**: 359–365.
- Bánész L.** (1994) Osídlenie územia v praveku. In: *Slovenský Kras* (eds. M. Rozložník and A. Karasová): 259–273. Osveta, Martin.
- Bárta J.** (1994) Jaskyne a človek. In: *Slovenský Kras* (eds. M. Rozložník and A. Karasová): 245–255. Osveta, Martin.
- Bella P.** (2003) Morphology and genesis of the Gombasecká Cave (in Slovak with English summary). *Slovenský Kras*, **41**: 47–68.
- Bíl M., Kubeček J.** (2012) Piping in loess-like and loess-derived soils: case study of Halenkovice site, Czech Republic. *Annales Societatis Geologorum Poloniae*, **82**: 45–50.
- Blikra L., Nemeč W.** (1998) Postglacial colluvium in western Norway: depositional processes, facies and palaeoclimatic record. *Sedimentology*, **45**: 909–959.
- Brock F., Higham T., Ditchfield P., Bronk Ramsey P.** (2010) Current pretreatment methods for AMS radiocarbon dating at the Oxford Radiocarbon Accelerator Unit (ORAU). *Radiocarbon*, **52**: 103–112.
- Bronk Ramsey C.** (2009) Bayesian analysis of radiocarbon dates. *Radiocarbon*, **51**: 337–360.
- Capezzuoli E., Gandin A., Sandrelli F.** (2010) Calcareous tufa as indicators of climatic variability: a case study from southern Tuscany (Italy). *Geological Society Special Publications*, **336**: 263–281.
- Carthew K.D., Drysdale R.N.** (2003) Late Holocene fluvial change in a tufa-depositing stream: Davys Creeek, New South Wales, Australia. *Australian Geographer*, **34**: 123–139.
- Carthew K.D., Taylor M.P., Drysdale R.N.** (2003) Are current models of tufa sedimentary environments applicable to tropical systems? A case study from Gregory River. *Sedimentary Geology*, **162**: 199–218.
- Czernik J., Goslar T.** (2001) Preparation of graphite targets in the Gliwice Radiocarbon Laboratory for AMS (super 14) C dating. *Radiocarbon*, **43**: 283–291.
- Drysdale R.N.** (1999) The sedimentological significance of hypsychid caddis-fly larvae (order: Trichoptera) in a travertine-depositing stream: Louie Creek, northwest Queensland, Australia. *Journal of Sedimentary Research*, **69**: 145–150.
- Drysdale R., Gillieson D.** (1997) Micro-erosion meter measurements of travertine deposition rates: a case study from Louie Creek, Northwest Queensland, Australia. *Earth Surface Processes and Landforms*, **22**: 1037–1051.
- Emeis K.-C., Richnow H.-H., Kempe S.** (1987) Travertine formation in Plitvice National Park, Yugoslavia: chemical versus biological control. *Sedimentology*, **34**: 595–609.
- Florsheim J.L., Ustin S.L., Tang Y., Di B., Huang C., Qiao X., Peng H., Zhang M., Cai Y.** (2013) Basin-scale and travertine dam-scale controls on fluvial travertine, Jiuzhaigou, southwestern China. *Geomorphology*, **180–181**: 267–280.
- Ford D.C., Williams P.W.** (2007) *Karst Hydrogeology and Geomorphology*. Wiley, Chichester.
- Ford T.D., Pedley H.M.** (1996) A review of tufa and travertine deposits of the world. *Earth-Sciences Reviews*, **41**: 117–175.
- Gandin A., Capezzuoli E.** (2008) Travertine versus calcareous tufa: distinctive petrologic features and stable isotopes signatures. *Italian Journal of Quaternary Sciences*, **21**: 125–136.
- García-García F., Pla-Pueyo S., Nieto L.M., Viseras, C.** (2013) Sedimentology of geomorphologically controlled tufas in a valley in southern Spain. *Facies* (in print) doi: 10.1007/s10347-013-0361-5
- Garnett E.R., Andrews J.E., Preece R.C., Dennis P.F.** (2004) Climatic change recorded by stable isotopes and trace elements in a British Holocene tufa. *Journal of Quaternary Science*, **19**: 251–256.
- Glover C., Robertson A.F.H.** (2003) Origin of tufa (cool water carbonate) and related terraces in the Antalya area, SW Turkey. *Geological Journal*, **38**: 329–358.
- Golubić S.** (1969) Cyclic and noncyclic mechanisms in the formation of travertine. *Internationale Vereinigung für Theoretische und Angewandte Limnologie*, **17**: 956–961.
- Goodfriend G.A., Stipp J.J.** (1983) Limestone and the problem of radiocarbon dating of land-snail shell carbonate. *Geology*, **11**: 575–577.
- Goslar T., Czernik J., Goslar E.** (2004) Low-energy ¹⁴C AMS in Poznań Radiocarbon Laboratory. *Nuclear Instruments and Methods B: 223–224*: 5–11.
- Goudie A.S., Viles H.A., Pentecost A.** (1993) The late-Holocene tufa decline in Europe. *Holocene*, **3**: 181–186.
- Gradziński M.** (2008) Origin of a unique tree-mould type cave in travertine based on examples from the village of Lúčky (Liptov, Slovakia). *Slovenský Kras*, **46**: 325–331.
- Gradziński M.** (2010) Factors controlling growth of modern tufa: results of a field experiment. *Geological Society Special Publications*, **336**: 143–191.
- Gradziński M., Szulc J., Motyka J., Stworzewicz, E., Tyc A.** (2001) Travertine mound and cave in a village of Laski, Silesian-Cracow Upland. *Annales Societatis Geologorum Poloniae*, **71**: 115–123.
- Gradziński M., Chmiel M.J., Lewandowska A., Michalska-Kasperkiewicz B.** (2010) Siliciclastic microstromatolites in a sandstone cave: role of trapping and binding of detrital particles in formation of cave deposits. *Annales Societatis Geologorum Poloniae*, **80**: 303–314.
- Harris P.M., Ellis, J., Purkis S.J.** (2013) Assessing the extent carbonate deposition in early rift settings. *AAPG Bulletin*, **97**: 17–60.
- Haviarová D., Fláková R., Seman M., Gaálová B., Ženišová Z.** (2012) Chemical composition and microbiological properties of karst waters of Silica-Gombasek cave system (Silická Plateau, Slovak Karst) (in Slovak with English summary). *Aragonit*, **17**: 3–14.
- Hercman H., Pawlak J.** (2012) MOD-AGE: An age-depth model construction algorithm. *Quaternary Geochronology*, **12**: 1–10.
- Hill C., Forti P.** (1997) *Cave Minerals of the World*. National Speleological Society, Huntsville.
- Hochstetter F.** (1856) Über die geologische Beschaffenheit der Umgegend von Edelény bei Miskolcz in Ungarn. *Jahrbuch der Kaiserlich-Königlichen Geologischen Reichsanstalt*, **7**: 692–705.
- Ihlenfeld Ch., Norman M.D., Gagan M.K., Drysdale R.N., Maas R., Webb J.** (2003) Climatic significance of seasonal trace element and stable isotope variations in a modern freshwater tufa. *Geochimica et Cosmochimica Acta*, **67**: 2241–2357.
- Irion G., Müller G.** (1968) Mineralogy, petrology and chemical composition of some calcareous tufa from the Schwäbische Alb, Germany. In: *Carbonate Sedimentology in Central Europe* (eds. G. Müller and G.M. Friedman): 157–171. Springer, New York.
- Jakál J., Bella P.** (2008) Water – creative agent of karst and caves. In: *Caves of the World Heritage in Slovakia* (eds. J. Jakál and P. Bella): 25–36. State Nature Conservancy of the Slovak Republic, Liptovský Mikuláš.
- Janssen A., Swennen R., Podoor N., Keppen E.** (1999) Biological and diagenetic influence in Recent and fossil tufa deposits from Belgium. *Sedimentary Geology*, **126**: 75–95.
- Jones B., Renaut R.W.** (2010) Calcareous spring deposits in continental settings. *Developments in Sedimentology*, **61**: 177–224.
- Keppel M.N., Clarke J.D.A., Halihan T., Love A.J., Werner A.D.** (2011) Mound springs in the arid Lake Eyre South region of South Australia: A new depositional tufa model and its controls. *Sedimentary Geology*, **240**: 55–70.
- Kilík J.** (2008) Calcareous tufa in Slovak Karst (in Slovak with English summary). *Naturae Tutela*, **12**: 177–184.

- Kormos T.** (1912) Beiträge zur Kenntnis der pleistozänen Molluskenfauna des Mittelkarpathen-Gebietes. Jahrbuch der Königlich ungarischen geologischen Reichsanstalt, [for 1910]: 326–340.
- Kovanda J.** (1971) Quaternary limestones of Czechoslovakia (in Czech with English summary). Sbornik Geologických Věd, Antropozoikum, **7A**: 7–256.
- Krapiec M., Walanus A.** (2011) Application of the triple-photomultiplier liquid spectrometer Hidex 300SL in radiocarbon dating. Radiocarbon, **53**: 543–550.
- Krippel E.** (1957) Ein Beitrag zur Entwicklung des Waldes im Gebiete des südslowakischen Karstes (in Slovak with German summary). Biológia, **12**: 884–893.
- Limondin-Lozouet N., Preece R.C.** (2004) Molluscan successions from the Holocene tufa of St Germain-le-Vasson, Normandy (France) and their biogeographical significance. Journal of Quaternary Science, **19**: 55–71.
- Ložek V.** (1955) Mollusken des tschechoslovakischen Quartärs (in Czech with German summary). Rozpravy Ústředního Ústavu Geologického Československé Akademie Věd, **17**: 475–495.
- Ložek V.** (1958) Stratigraphie und Weichtiere der holozänen Travertine in Háj bei Turňa (in Czech with German summary). Anthropozoikum, **7**: 27–36.
- Ložek, V., Prošek F.** (1956) Über Veränderungen des Landschaftsbildes des Südslowakischen Karstes in der jüngsten geologischen Vergangenheit (in Czech with German summary). Ochrana Přírody, **11**: 33–42.
- Martín-Algarra A., Martín-Martín M., Andreo B., Julià R., González-Gómez C.** (2003) Sedimentary patterns in perched spring travertines near Granada (Spain) as indicators of the palaeohydrological and palaeoclimatological evolution of a karst massif. Sedimentary Geology, **161**: 217–228.
- Mastella L., Rybak-Ostrowska B.** (2012) Tectonic control of tufa occurrences in the Polish Synclinorium (Central Western Carpathians, southern Poland). Geological Quarterly, **56** (4): 733–744.
- Mello J., ed.** (1996) Geological map of the Slovenský Kras Mts. Ministerstvo Životného Prostredia Slovenskej Republiky. Geologická Služba Slovenskej Republiky, Bratislava.
- Merz-Preiß M., Riding R.** (1999) Cyanobacterial tufa calcification in two freshwater streams: ambient environment, chemical thresholds and biological processes. Sedimentary Geology, **126**: 103–124.
- Meyrick R.A.** (2003) Holocene molluscan faunal history and environmental change at Kloster Mühle, Rheinland-Pfalz, western Germany. Journal of Quaternary Science, **18**: 121–132.
- Meyrick R.A., Preece R.C.** (2001) Molluscan successions from two Holocene tufas near Northampton, English Midlands. Journal of Biogeography, **28**: 77–93.
- Moyersons J., Nyssen J., Poesen J., Deckers J., Haile M.** (2006) Age and backfill/overflow stratigraphy of two tufa dams, Tigray Highlands, Ethiopia: Evidence for late Pleistocene and Holocene wet conditions. Palaeogeography, Palaeoclimatology, Palaeoecology, **230**: 165–181.
- Němejc F.** (1936) The palaeobotanical researches in the travertine deposits of the Slovakian Karst. Bulletin International de l'Académie des Sciences de Bohême: 1–47.
- Němejc F.** (1944) Výsledky dosavadních výzkumů paleobotanických v kvarteru západního dílu karpatského obluku. Rozpravy II. Třída České Akademie, **53** (35): 1–47.
- Ordóñez S., García del Cura M.A.** (1983) Recent and Tertiary fluvial carbonates in Central Spain. IAS Special Publication, **6**: 485–497.
- Ordóñez S., González Martín J.A., García del Cura M.A., Pedley H.M.** (2005) Temperate and semi-arid tufas in the Pleistocene to Recent fluvial barrage system in the Mediterranean area: the Ruidera Lakes Natural Park (Central Spain). Geomorphology, **69**: 332–350.
- Pazdur A., Pazdur M.F., Starkel L., Szulc J.** (1988a) Stable isotopes of Holocene tufa in Southern Poland as paleoclimatic indicator. Quaternary Research, **30**: 177–189.
- Pazdur A., Pazdur M.F., Szulc J.** (1988b) Radiocarbon dating of Holocene calcareous tufa in southern Poland. Radiocarbon, **30**: 133–152.
- Pedley H.M.** (1987) The Flandrian (Quaternary) Caerwys Tufa, North Wales: an ancient barrage tufa deposit. Proceedings of the Yorkshire Geological Society, **46**: 141–152.
- Pedley H.M.** (1990) Classification and environmental models of cool freshwater tufas. Sedimentary Geology, **68**: 143–154.
- Pedley M.** (1992) Freshwater (phytoherm) reefs: the role of biofilms and their bearing on marine reef cementation. Sedimentary Geology, **79**: 255–274.
- Pedley H.M.** (1993) Sedimentology of the late Quaternary barrage tufas in the Wye and Lathkill valleys, north Derbyshire. Proceedings of the Yorkshire Geological Society, **49**: 197–206.
- Pedley M.** (2009) Tufas and travertines of the Mediterranean region: a testing ground for freshwater carbonate concepts and developments. Sedimentology, **56**: 221–246.
- Pedley M., Andrews J., Ordóñez S., García del Cura M.A., González Martín J.A., Taylor D.** (1996) Does climate control the morphological fabric of freshwater carbonates? A comparative study of Holocene barrage tufas from Spain and Britain. Palaeogeography, Palaeoclimatology, Palaeoecology, **121**: 239–257.
- Pedley M., González Martín J.A., Ordóñez Delgado S., García del Cura A.G.** (2003) Sedimentology of Quaternary perched springline and paludal tufas: criteria for recognition, with examples from Guadalajara Province, Spain. Sedimentology, **50**: 23–44.
- Pedley M., Rogerson M., Middleton R.** (2009) Freshwater calcite precipitates from *in vitro* mesocosm flume experiments: a case for biomediation of tufas. Sedimentology, **56**: 511–527.
- Peña J.L., Sancho C., Lozano M.V.** (2000) Climatic and tectonic significance of Late Pleistocene and Holocene tufa deposition in the Miojares River canyon, Eastern Iberian Range, northeastern Spain. Earth Surface Processes and Landforms, **25**: 1403–1417.
- Pentecost A.** (1998) The significance of calcite (travertine) formation by algae in a moss-dominated travertine from Matlock Bath, England. Archiv für Hydrobiologie, **143**: 487–509.
- Pentecost A.** (1999) The origin and development of the travertines and associated thermal waters at Matlock Baths, Derbyshire. Proceedings of the Geologists' Association, **110**: 217–232.
- Pentecost A.** (2005) Travertine. Springer, Berlin.
- Pentecost A., Viles H.** (1994) A review of reassessment of travertine classification. Géographie Physique et Quaternaire, **48**: 305–314.
- Pentecost A., Whitton B.A.** (2000) Limestones. In: The Ecology of Cyanobacteria (eds. B.A. Whitton and M. Potts): 257–279. Kluwer, Amsterdam.
- Pentecost A., Zhang Z.** (2001) A review of Chinese travertines. Cave and Karst Science, **28**: 15–28.
- Petrbok J.** (1937) Mekkýši travertínů slovenského Krasu, Gánovců s okolím, Spiše a Ružbachů. Rozpravy II. Třída České Akademie, **46** (5): 1–16.
- Pigati J.S., Rech J.A., Nekola J.C.** (2010) Radiocarbon dating of small terrestrial gastropod shells in North America. Quaternary Geochronology, **5**: 519–532.
- Preece R.C., Bridgland D.R.** (1999) Holywell Coombe, Folkestone: A 13,000 year history of an English Chalkland Valley. Quaternary Science Reviews, **18**: 1075–1125.
- Preece R.C., Day S.P.** (1994) Comparison of Post-glacial molluscan and vegetational successions from a radiocarbon-dated tufa sequence in Oxfordshire. Journal of Biogeography, **21**: 463–478.
- Reimer P.J., Baillie M.G.L., Bard E., Bayliss A., Beck J.W., Blackwell P.G., Bronk Ramsey C., Buck C.E., Burr G.S., Edwards R.L., Friedrich M., Grootes P.M., Guilderson T.P., Hajdas I., Heaton T.J., Hogg A.G., Hughen K.A., Kaiser K.F., Kromer B., McCormac F.G., Manning S.W., Reimer R.W., Richards D.A., Southon J.R., Talamo S., Turney C.S.M., van der Plicht J., Weyhenmeyer C.E.** (2009). IntCal09 and Marine09 radiocarbon age calibration curves, 0–50,000 years cal BP. Radiocarbon, **51**: 1111–1150.

- Sanders D., Wertl W.** (2011) Spring-associated limestones of the Eastern Alps: overview of facies, deposystems, minerals, and biota. *Facies*, **57**: 395–316.
- Scott A.C.** (2010) Charcoal recognition, taphonomy and uses in palaeoenvironmental analysis. *Palaeogeography, Palaeoclimatology, Palaeoecology*, **291**: 11–39.
- Shiraishi F., Reimer A., Bissett A., Beer D. de, Arp G.** (2008) Microbial effects on biofilm calcification, ambient water chemistry and stable isotope records in a highly supersaturated setting (Westerhöfer Bach, Germany). *Palaeogeography, Palaeoclimatology, Palaeoecology*, **262**: 91–106.
- Soják M.** (2007) Osídlenie blízkeho okolia Moldavy nad Bodvou. In: *Moldavská jaskyňa v zrkadle dejín* (eds. M. Soják and M. Terray): 50–72. Mestský úrad v Moldave nad Bodvou, Moldava nad Bodvou.
- Soják M.** (2008) Cave settlement. In: *Caves of the World Heritage in Slovakia* (eds. J. Jakál and P. Bella): 109–122. State Nature Conservancy of the Slovak Republic, Liptovský Mikuláš.
- Soligo M., Tuccimei P., Barberi R., Delitala M.C., Miccadei E., Tadeucci A.** (2002) U/Th dating of freshwater travertine from Middle Velino Valley (Central Italy): paleoclimatic and geologic implications. *Palaeogeography, Palaeoclimatology, Palaeoecology*, **184**: 147–161.
- Steidtmann E.** (1936) Travertine-depositing waters near Lexington, Virginia. *Journal of Geology*, **44**: 193–200.
- Stuiver M., Polach H.A.** (1977) Discussion. Reporting of ¹⁴C data. *Radiocarbon*, **19**: 355–363.
- Sürmelihindli G., Passchier C.W., Spötl Ch., Kessner P., Bestmanns M., Jacob D., Baykan O.N.** (2013) Laminated carbonate deposits in Roman aqueducts: Origin, processes and implications. *Sedimentology*, **60**: 961–982.
- Szulc J.** (1983) Genesis and classification of calcareous sinter deposits (in Polish with English summary). *Przegląd Geologiczny*, **31**: 231–237.
- Szulc J.** (1984) Sedymentacja czwartorzędowych martwic wapiennych Polski południowej. PhD thesis. Polska Akademia Nauk, Instytut Nauk Geologicznych.
- Šemnički P., Previšić A., Ivković M., Čmrlec K., Mihajlevic Z.** (2012) Tufa barriers from a caddisfly's point of view. Streams or lake outlets? *International Review of Hydrobiology*, **97**: 465–484.
- Taylor D.M., Pedley H.M., Davies P., Wright M.W.** (1998) Pollen and mollusc records for environmental change in central Spain during the mid- and late Holocene. *Holocene*, **8**: 605–612.
- Turner E.C., Jones B.** (2005) Microscopic calcite dendrites in cold-water tufa: implications for nucleation of micrite and cement. *Sedimentology*, **52**: 1043–1066.
- Vázquez-Urbez M., Arenas C., Pardo G.** (2012) A sedimentary facies model for stepped, fluvial tufa system in the Iberian Range (Spain): the Quaternary Piedra and Mesa valleys. *Sedimentology*, **61**: 502–526.
- Vázquez-Urbez M., Arenas C., Padro G., Pérez-Rivarés S.** (2013) The effect of drainage reorganization and climate on the sedimentologic evolution of intermontane lake systems: The final fill stage of the Tertiary Ebro Basin (Spain). *Journal of Sedimentary Research*, **83**: 562–590.
- Vermoere M., Degryse P., Vanhecke L., Muchez Ph., Palulissen E., Smets E., Waelkens M.** (1999) Pollen analysis of two travertine sections in Basköy (southwestern Turkey): implications for environmental conditions during the early Holocene. *Review of Palaeobotany and Palynology*, **105**: 93–110.
- Verrecchia E.P., Freydet P., Julien J., Baltzer F.** (1997) The unusual hydrodynamic behaviour of freshwater oncolites. *Sedimentary Geology*, **113**: 225–243.
- Viles H.A., Naylor L.A., Carter N.E.A., Chaput D.** (2008) Biogeomorphological disturbance regimes: progress in linking ecological and geomorphological systems. *Earth Surface Processes and Landforms*, **33**: 1419–1435.
- Viles H.A., Pentecost A.** (2007) Tufa and travertine. In: *Geochemical Sediments & Landscapes* (eds. D.J. Nash and S.J. McLaren): 173–199. Blackwell, Malden.
- Viles H.A., Taylor M.P., Nicoll K., Neumann S.** (2007) Facies evidence of hydroclimatic regime shifts in tufa depositional sequences from the arid Naukluft Mountains, Namibia. *Sedimentary Geology*, **195**: 39–53.
- Violante C., Ferreri V., D'Argenio B., Golubic S.** (1994) Quaternary travertines at Rocchetta a Volturno (Insernia, Central Italy). Facies analysis and sedimentary model of an organogenic carbonate system. In: *Pre Meeting Fieldtrip Guidebook, 15th Regional Meeting of International Association of Sedimentologists, Ischia* (eds. G. Carannante and R. Tonielli): 3–23. International Association of Sedimentologists.
- Vitális S.** (1909) Die geologischen Verhältnisse der Umgebung des Bodva und Tornabaches. *Jahresbericht der Königlich Ungarischen Geologischen Reichsanstalt*, [for 1907]: 50–66.
- Walker D.** (2007) Holocene sediments of Lake Barrine, north-east Australia, and their implications for the history of lake and catchment environments. *Palaeogeography, Palaeoclimatology, Palaeoecology*, **251**: 57–82.
- Weijermars R., Mulder-Blanken C.W., Wieggers J.** (1986) Growth rate observation from the moss-built Checa travertine terrace, central Spain. *Geological Magazine*, **123**: 279–286.
- Whitlock C., Millspaugh S.H.** (1996) Testing the assumption of fire history studies: An examination of modern charcoal accumulation in Yellowstone National Park, USA. *Holocene*, **6**: 7–15.
- Zambo L., Ford D.C.** (1997) Limestone dissolution processes in Beke Doline Aggtelek National Park, Hungary. *Earth Surface Processes and Landforms*, **22**: 531–543.
- Žák K., Ložek V., Kadlec J., Hladíkova J., Čílek V.** (2002) Climate-induced changes in Holocene calcareous tufa formations, Bohemian Karts, Czech Republic. *Quaternary International*, **91**: 137–152.